

2015

## GELATIN MICROGEL INCORPORATED POLY (ETHYLENE GLYCOL) BIOADHESIVE WITH ENHANCED ADHESIVE PROPERTY AND BIOACTIVITY

Yuting Li  
*Michigan Technological University*

Follow this and additional works at: <https://digitalcommons.mtu.edu/etds>

 Part of the [Biomedical Engineering and Bioengineering Commons](#)

Copyright 2015 Yuting Li


---

### Recommended Citation

Li, Yuting, "GELATIN MICROGEL INCORPORATED POLY (ETHYLENE GLYCOL) BIOADHESIVE WITH ENHANCED ADHESIVE PROPERTY AND BIOACTIVITY", Master's Thesis, Michigan Technological University, 2015.

<https://digitalcommons.mtu.edu/etds/999>

Follow this and additional works at: <https://digitalcommons.mtu.edu/etds>

 Part of the [Biomedical Engineering and Bioengineering Commons](#)

GELATIN MICROGEL INCORPORATED POLY (ETHYLENE GLYCOL)  
BIOADHESIVE WITH ENHANCED ADHESIVE PROPERTY AND BIOACTIVITY

By

Yuting Li

A THESIS

Submitted in partial fulfillment of the requirements for the degree of

MASTER OF SCIENCE

In Biomedical Engineering

MICHIGAN TECHNOLOGICAL UNIVERSITY

2015

© 2015 Yuting Li

This thesis has been approved in partial fulfillment of the requirements for the Degree of MASTER OF SCIENCE in Biomedical Engineering.

Department of Biomedical Engineering

Thesis Advisor: *Bruce P. Lee*

Committee Member: *Feng Zhao*

Committee Member: *Ching-An Peng*

Department Chair: *Sean J. Kirkpatrick*

## Contents

List of Figures.....	5
List of Tables.....	7
Acknowledgements.....	8
Abstract.....	10
1. Introduction.....	12
1.1 Tissue adhesive.....	15
1.2 DOPA.....	17
1.3 Poly(ethylene glycol).....	21
1.4 Gelatin.....	23
1.5 Wound healing.....	25
2. Experimental.....	27
2.1 Materials.....	27
2.2 Methods.....	28
2.2.1 Synthesis of dopamine-modified 8-arm PEG (PEGDM).....	28
2.2.2 Preparation of gelatin microgel.....	30
2.2.3 Preparation and characterization of gelatin microgel incorporated PEG (PEG-GM) adhesive.....	31
2.2.4 Mechanical properties.....	33
2.2.4.1 Compression test.....	33
2.2.4.2 Oscillatory rheometry.....	34
2.2.5 Lap shear test.....	34
2.2.6 <i>In vitro</i> degradation test.....	35
2.2.7 Cell experiment.....	36
2.2.7.1 Cell viability.....	36
2.2.7.2 Cell attachment.....	37
2.2.8 Subcutaneous implantation.....	38
2.2.9 Statistical analysis.....	39
3. Results and discussions.....	40

<b>3.1</b>	<b>Preparation and characterization of materials</b> .....	<b>40</b>
<b>3.2</b>	<b>Mechanical property test</b> .....	<b>45</b>
<b>3.2.1</b>	<b>Compression test</b> .....	<b>45</b>
<b>3.2.2</b>	<b>Oscillatory rheometry</b> .....	<b>46</b>
<b>3.3</b>	<b>Lap shear test</b> .....	<b>48</b>
<b>3.4</b>	<b><i>In vitro</i> degradation test</b> .....	<b>50</b>
<b>3.5</b>	<b>Cell experiment</b> .....	<b>51</b>
<b>3.5.1</b>	<b>Cell viability</b> .....	<b>51</b>
<b>3.5.2</b>	<b>Cell attachment</b> .....	<b>52</b>
<b>3.6</b>	<b>Subcutaneous implantation</b> .....	<b>55</b>
<b>4.</b>	<b>Conclusion</b> .....	<b>63</b>
<b>5.</b>	<b>Future work</b> .....	<b>64</b>
<b>6.</b>	<b>Reference</b> .....	<b>66</b>
	<b>Appendix</b> .....	<b>72</b>

## List of Figures

Figure 1-1. Schematic illustration of the reactions between dopamine-modified PEG and gelatin microgel or native tissue. Catechol groups are oxidized to form reactive quinones A) the highly reactive quinones interact with each other to complete the polymerization of adhesive; B) highly reactive quinones interact with gelatin microgel to form covalent bonds; C) highly reactive quinones interact with native tissue and form covalent bond. ....	14
Figure 1-2. Chemical structure of DOPA. A catechol group shows in the side-chain of the DOPA structure.....	18
Figure 1-3. Image and schematic illustration of mussel structure. A) Adult mussel with radially extended byssus attaching on a solid surface; B) Schematic representation of the mussel with byssus consists of threads and plaques and attaches to the stem. <sup>[32]</sup> (Copyright permission documentation in Appendix).....	18
Figure 1-4. Schematic of catechol group reactions. A) catechol groups form reversible bond with metal ion; B) catechol groups react with metal oxide surface to form reversible bond; catechol groups oxidized into highly reactive quinones C) quinones react with each other to complete the polymerization; D) or react with different functional groups showing on the tissue surface to form covalent bond. ....	20
Figure 1-5. Synthesis of poly (ethylene glycol) from anionic polymerization of ethylene oxide. ....	21
Figure 1-6. Schematic illustration of EDC/NHS involved chemical crosslinking. <sup>[62]</sup> –COOH and –NH <sub>2</sub> groups in gelatin structure form covalent bond to chemically crosslink the gelatin hydrogel under the function of EDC and NHS. Reprinted with permission from [60]. Copyright (1999) American Chemical Society. (Copyright permission documentation in Appendix).....	25
Figure 2-1. Image of the experiment to determine the cure time of adhesive. The cure time was determined when the adhesive solution stopped flow in a tilt vial. 8.....	32
Figure 2-2. Photographs of preparation for lap shear test. A) One piece of bovine pericardium placed in a mold; B) the other piece of bovine pericardium placed on a glass slide; C) adhesive precursor solutions was mixed in the overlap area; D) the mixed precursor solution covered by the other piece of bovine pericardium; E) 100g weigh loaded on the overlap area for 10min. ....	35
Figure 3-1. SEM image of gelatin microgel.....	43
Figure 3-2. Cure time of PEG-GM adhesive with different gelatin microgel weight percentage. The cure time decreased with the increasing weight percentage of gelatin microgel. * p < 0.05 when compared with 0wt% adhesive.....	43
Figure 3-3. FTIR results of PEGDM adhesive (black) and PEG-GM adhesive (red). ....	44
Figure 3-4. Equilibrium water content of PEG-GM adhesive with different gelatin microgel weight percentage. The equilibrium water content decreased with increasing weight percentage of gelatin microgel. * p < 0.05 when compared with 0wt% adhesive; # p < 0.05 when compared with 1.5wt% adhesive; § p < 0.05 when compared with 3.75wt% adhesive.....	44
Figure 3-5. Storage and loss modulus of PEG-GM adhesive. The storage modulus and loss	

modulus increased with the increasing weight percentage of gelatin microgel. ....	48
Figure 3-6. Lap shear adhesion test results of PEG-GM adhesive with different weight percentage of gelatin microgel. * $p < 0.05$ when compared to 0wt% adhesive. # $p < 0.05$ when compared to 1.5wt% adhesive. ....	49
Figure 3-7. <i>In vitro</i> degradation test of PEG-GM adhesives containing 0wt%, 1.5wt%, 3.75wt% and 7.5wt% gelatin microgels. ....	50
Figure 3-8. Relative cell viability test results of PEG-GM adhesives containing 0wt%, 3.75wt% and 7.5wt% gelatin microgel.....	52
Figure 3-9. Cell attachment result. The number of attached rat dermal fibroblasts on the adhesive increased with the increased weight percentage of gelatin microgel.* $p < 0.05$ when compared to...	54
Figure 3-10. Live/dead staining result of cell attachment test. Cells spread better with increasing weight percentage of gelatin microgel. A: 0wt% adhesive; B: 3.75wt% adhesive; C: 7.5wt% adhesive . Living cells were stained in green and dead cells were stained in red. Gelatin microgels were also stained into green through non-specific binding. Blue arrow: gelatin microgel; Red arrow: spread cells; Orange arrow: dead cells; Yellow arrow: Living cells but not spread.....	55
Figure 3-11. Hematoxylin and eosin stain (H&E stain) (A and B), Masson's Trichrome stain (C and D) and immunofluorescent stain (E-J) of 0wt% and 7.5wt% adhesive and surrounding tissue after 2 weeks subcutaneous implantation. a: adhesive; Orange box: cell distribution area. Single headed arrow: cell infiltrating into the pocket formed via gelatin microgel degradation. Blue (DAPI): cell nuclei; Green (CD11b): M1 macrophage; Red (CD163 and S100A4): M2 macrophage and fibroblast, respectively.....	60
Figure 3-12. Hematoxylin and eosin stain (H&E stain) (A and B), Masson's Trichrome stain (C and D) and immunofluorescent stain (E-H) of 0wt% and 7.5wt% adhesive and surrounding tissue after 6 weeks subcutaneous implantation. a: adhesive; Orange box: cell distribution area. Single headed arrow: cell infiltrating into the pocket formed via gelatin microgel degradation. Double headed arrow : cell infiltration layer (IL in A and B) and collagen layer (CL in C and D), respectively. Blue (DAPI): cell nuclei; Green (CD11b): M1 macrophage; Red (CD163 and S100A4): M2 macrophage and fibroblast, respectively.....	62

# List of Tables

Table 3-1. Compression test results of 0wt%, 1.5wt%, 3.75wt% and 7.5wt% PEG-GM adhesive. .45  
Table 3-2. Cell density, cell infiltration layer and collagen layer thickness of 2 weeks and 6 weeks subcutaneous implantation. ....63



## **Acknowledgements**

This project was supported by National Institute of Health and Kenneth L. Stevenson Biomedical Engineering Summer Research Fellowship.

I would like to thank my advisor Professor Bruce P. Lee for his support, encouragement and patience throughout my graduate education. His professional advice was essential to the completion of this thesis. His serious attitude to science and passions towards work educated me what a master scientist should be. He also taught me a lot about life as an elder friend. I feel fortunate to have him as my advisor and life-long friend.

My thanks also go to my committee members Professors Feng Zhao and Ching-An Peng for their valuable suggestions on my thesis and discussions during my oral defense.

I also appreciate the help from my labmates and friends. Hao Meng and Yuan Liu are the two most important friends of mine in the lab. They provided me training on mechanical testing, cell experiment and animal experiment as well as many helpful discussions.

Thank Ameya Narkar, who helped me on the rheological tests. Thank Rattapol Pinnaratip and Madeline Faust for their kind help in my experiment.

At last, I would like to thank my dear husband Yang. His understanding, love,

encouragement and support make this thesis possible. He is a good husband, a good friend and will soon be a good father.

## Abstract

In this study, chemically crosslinked gelatin microgels were incorporated into dopamine-modified poly (ethylene glycol) (PEGDM) adhesive to form composite bioadhesive with simultaneously improved adhesive property and bioactivity. Gelatin microgel, with an average diameter of  $53.6 \pm 14.2 \mu\text{m}$ , was prepared with water in oil emulsification method and chemically crosslinked with 1-ethyl-3-[3-dimethylaminopropyl]carbodiimide hydrochloride (EDC) and N-hydroxysuccinimide (NHS). Gelatin microgels were incorporated into PEGDM adhesive precursor solution at 1.5wt%, 3.75wt% and 7.5wt%. The cure time of adhesive reduced from 54 seconds to 37 seconds with increasing gelatin microgel content. Additionally, the incorporation of the gelatin microgel also increased the crosslinking density of the adhesive network as indicated by the reduced equilibrium water content and increased elastic modulus based on compression testing. The compliance of adhesive was not compromised with the increased crosslinking density, as the failure strain showed no significant decrease from the compression testing result. Results from oscillator rheometry indicated that both the storage and loss moduli of the adhesive increased with increasing microgel content, which suggested that the microgels increased both chemical and physical crosslinks in the adhesive architecture. The increased physical crosslink indicated increased energy dissipation ability of the

adhesive. Lap shear adhesive test demonstrated that the addition of gelatin microgel enhanced the adhesive property of adhesive. The adhesive property was increased 1.5-2 fold after the addition of gelatin microgel. In the *in vitro* degradation test, samples of different formulation groups degraded gradually under a similar rate after soaked in the phosphate buffer solution (pH=7.4) and incubated at 37°C. After 8 weeks samples were completely degraded. The *in vitro* cell viability was tested with L929 mouse fibroblast and the results showed no cytotoxicity in each test formulation. The *in vitro* cell attachment experiment revealed an enhanced cell attachment and spreading of primary rat dermal fibroblast on gelatin microgel containing PEGDM adhesive compared to the adhesive without gelatin microgel. The results of rat subcutaneous implantation revealed higher cell recruitment and collagen deposition compared with control adhesive group which has no gelatin microgel in structure. Cell infiltration was found in the pocket structure formed by the degradation of gelatin microgel. In conclusion, the incorporation of gelatin microgel presents a simple method to simultaneously enhance the adhesive property and bioactivity of bioadhesive.

# 1. Introduction

Surgical sutures, staples and clips are traditionally used in wound closure and tissue reconstruction. But these methods present many drawbacks such as causing chronic pain and additional damage to wound.<sup>[1]</sup> Bioadhesives as an alternative choice has attracted more and more attention during the past decades. It can be delivered with minimally invasive method and gel *in situ*. The bioadhesives adhere to the native tissue and hold the edges of the wound together to promote wound closure without introducing extra damage and pain suffering. However, bioadhesives in the current market present many limitations, such as the risk of disease transmission, poor adhesive strength (e.g., fibrin glue)<sup>[2]</sup>, cytotoxicity (e.g., cyanoacrylate adhesive) and lacking bioactivity (poly(ethylene glycol) (PEG)-based adhesive).

Poly (ethylene glycol) (PEG)-based bioadhesives have been widely investigated due to their tunable properties, cytocompatibility and bioinert property as well as high water content which is similar to the extracellular environment of tissue.<sup>[3]</sup> However, the bioinert property makes PEG-based adhesives resisting to the cell adhesion and lacking interaction with surrounding cells to regulate the cell function.<sup>[4]</sup> Many studies have been performed to investigate the method to improve the interaction between cell and adhesives. For example, bioligands, such as cysteine-containing peptides or proteins,

have been tethered on the PEG structure to mimic the extracellular matrix (ECM) and interact with cell membrane receptor to modulate cell morphogenesis.<sup>[5]</sup> Other short peptide sequences presenting in ECM protein, such as Arg-Gly-Asp (RGD)<sup>[6]</sup> and Arg-Glu-Asp-Val (REDV)<sup>[7]</sup>, are also used to promote cell adhesion and proliferation. However, functionalizing PEG with bioactive peptide sequences requires multi-step chemical synthetic approach, which is associated with low yield and high cost. Most importantly, peptide-functionalization does not increase the mechanical properties of these materials.

Gelatin is hydrolyzed from collagen which is the main component of ECM and contains RGD sequence to promote cell adhesion, migration and proliferation.<sup>[8-11]</sup> Since it is derived from ECM, it shows nontoxicity and biodegradability.<sup>[12]</sup> The physical network of gelatin gel can easily break down at a higher temperature but the thermal and mechanical stability can be improved through chemical crosslinking.<sup>[13]</sup> The application of gelatin microgel has been reported in drug delivery<sup>[14]</sup> and tissue engineering<sup>[15]</sup>. Drug molecule was loaded in the gelatin microgel and released after delivered into physiological environment. Growth factor was also entrapped within the structure of gelatin microgel to promote the tissue regeneration.

In this project, we combined biomimetic PEG-based adhesive with gelatin microgel to prepare a novel bioadhesive with enhanced adhesive property and bioactivity. PEG is a hydrophilic and biocompatible polymer that serves as the backbone of the adhesive. The glutaric acid was linked with PEG through ester bond, which can be hydrolyzed in the presence of water. Dopamine was modified on the end of PEGGlu structure. The catechol groups can be oxidized by  $\text{NaIO}_4$  to form highly reactive quinones. The quinones subsequently react with each other to form covalent bonds completing the polymerization of adhesive (Figure 1-1A). Other quinones will react with amine groups in the gelatin microgel structure to form covalent bonds (Figure 1-1B) or with other functional groups in the tissue to form covalent bonds completing the adhesion to tissue surface (Figure 1-1C).

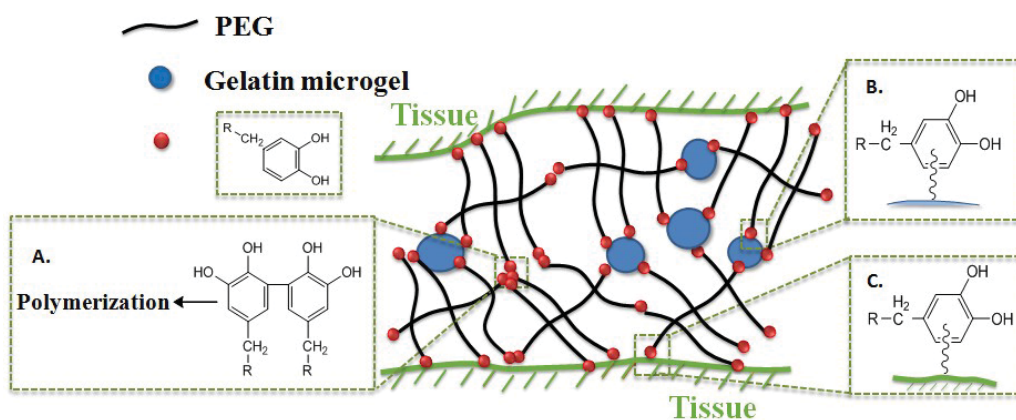


Figure 1-1. Schematic illustration of the reactions between dopamine-modified PEG and gelatin microgel native tissue. Catechol groups are oxidized to form reactive quinones A) the highly reactive quinones interact with each other to complete the polymerization of adhesive; B) highly reactive quinones interact with gelatin microgel to form covalent bonds; C) highly reactive quinones

interact with native tissue and form covalent bond.

## **1.1 Tissue adhesive**

The application of tissue adhesive for wound closure can minimize the trauma, reduce the operation time and effectively stop the leakage of body fluid. An ideal tissue adhesive is expected to possess following properties.<sup>[16]</sup> First, an ideal tissue adhesive should present sufficient flow characteristic when it is in the liquid state so that it can be applied easily on the tissue surface. Second, the ideal tissue adhesive should be able to solidify from liquid state rapidly under mild physiological condition. Third, after the gelation the adhesive should maintain strong adhesion to the tissue and strong bulk mechanical property during the healing phase. Finally, the adhesive should also be biocompatible and sterilized easily without compromising its properties. Current tissue adhesives can be classified into two categories: biological and synthetic adhesives.

Fibrin glue is a biological tissue adhesive and it has been investigated for decades. Fibrin glue mimics the final stage of blood clotting.<sup>[2]</sup> Fibrinogen and thrombin are the two main components involved in the process. By mimicking the blood clotting process, fibrinopeptides are removed from fibrinogen under the mediation of thrombin. After the removal of fibrinopeptides, fibrinogen changes the conformational structure and



self-assemble into fibrin gel to adhere on the surrounding tissue. The fibrin gel provides adhesion sites for cell migration and proliferation to promote the tissue regeneration.<sup>[17]</sup> Additionally, it also presents advantages such as controllable degradation to precisely match the rate of tissue regeneration, rapid hemostasis and excellent biocompatibility.<sup>[2]</sup> The fibrin sealants have been successfully used in a number of surgical practices, such as cardiovascular, neuro-, plastic, hernia repair<sup>[18]</sup> and liver surgeries<sup>[19]</sup>. However, the fibrinogen and thrombin are obtained from blood which makes the fibrin sealants at a risk of disease transmission. In addition, the relative low mechanical properties make fibrin sealants undesirable as a tissue adhesive.

Cyanoacrylate adhesive (CA) is synthesized through the condensation polymerization of cyanoacetate and formaldehyde.<sup>[20]</sup> It shows a relatively high bonding strength and has been used in various applications, such as vascular repair<sup>[21, 22]</sup>, hemostasis<sup>[23, 24]</sup> as well as retinal repair<sup>[25]</sup>. The adhesive provides a water-resistant barrier for wound but a constant exposure to body fluids may weaken the adhesive property.<sup>[26]</sup> Additionally, the CA adhesive causes inflammation *in vivo* and is toxic to the cells *in vitro*. Cell damage may be caused by the released heating during the polymerization process.<sup>[27]</sup>

Poly (ethylene glycol) (PEG)-based tissue adhesive is another important type of

synthetic adhesives. PEG-based tissue adhesive has been used in many biomedical applications because of its biocompatibility, non-immunogenicity, and bioinert characteristics to resist cells or proteins adsorption.<sup>[28]</sup> Crosslinked oxidized methacrylated alginate/PEG (OMA/PEG) hydrogel as bioadhesive has been studied by Jeon *et al.* recently. It has been demonstrated that by changing the degree of alginate oxidation, the swelling behavior, degradation and storage modulus of hydrogel are tunable.<sup>[29]</sup> The adhesion strength of OMA/PEG is also superior to the commercial fibrin glue. PEG end-functionalized with DOPA and its derivatives (e.g., dopamine, 3,4-dihydroxyhydrocinnamic acid) have been investigated as injectable tissue adhesive and sealant.<sup>[30]</sup> These adhesives outperformed fibrin glue in various adhesion tests, including lap shear, burst strength and peel adhesion tests. Brubaker *et al.*<sup>[31]</sup> endcapped PEG with catechol groups, which is a functional groups in DOPA and its derivatives, and used this novel tissue adhesive in extrahepatic islet transplantation. The adhesive hydrogel cured in 1min and elicited minimal inflammatory response in mice.

## **1.2 DOPA**

DOPA (3,4-dihydroxyphenylalanine) is a catechol-containing amino acid (Figure 1-2) which is found in the structure of mussel byssal plaque protein.<sup>[32]</sup> The byssus consists

of plaques, threads, stem and root. The byssus threads are rapidly made of proteins and radially distributed while attaching to the stem. The plaques are responsible for the attachment to the outside surfaces. (Figure 1-3)

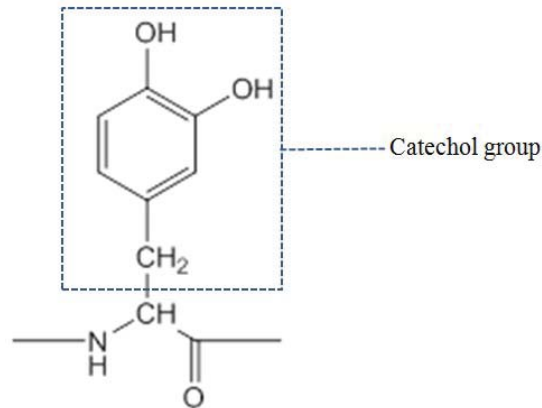


Figure 1-2. Chemical structure of DOPA. A catechol group shows in the side-chain of the DOPA structure.

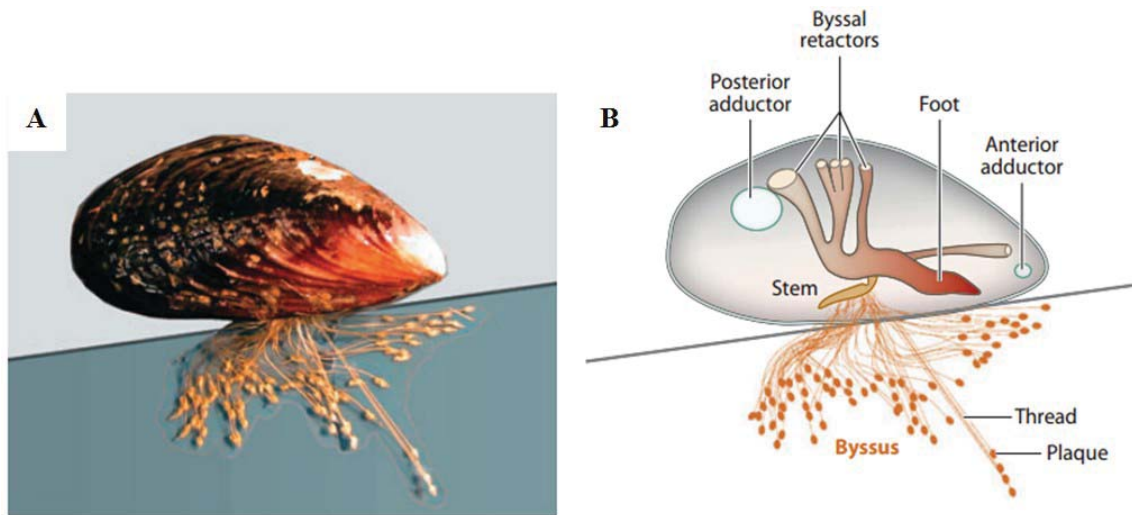


Figure 1-3. Image and schematic illustration of mussel structure. A) Adult mussel with radially extended byssus attaching on a solid surface; B) Schematic representation of the mussel with byssus consists of threads and plaques and attaches to the stem.<sup>[32]</sup> (Copyright permission documentation in Appendix)

The byssal plaques are believed to be responsible for the strong adhesive performance due to the high content of unique mussel foot proteins (Mfp-2, -3, -4, -5 and -6), which all contain DOPA. The catechol group of DOPA has the capability to undergo different catechol-catechol or catechol-surface interactions (Figure 1-4). Catechol groups can react with metal ions<sup>[33]</sup> (Figure 1-4A) or metal oxide surface<sup>[34]</sup> (Figure 1-4B) to form reversible bond. Catechol groups can be oxidized into highly reactive quinones and react with each other to complete the polymerization process<sup>[35]</sup> (Figure 1-4C). When quinones react with natural tissue, covalent bonds can be formed with the functional groups showing in the tissue, such as lysyl groups, cystainyl groups and histidyl groups<sup>[36, 37]</sup> (Figure 1-5D). Lee *et al.*<sup>[36]</sup> investigated the single-molecule adhesion of DOPA. The results suggested that the interaction between DOPA and wet inorganic surface is strong (~800pN) and reversible. However, the interaction between DOPA and amine-modified organic surface was dramatically higher than that between DOPA and inorganic surface. The 2.2nN force was believed coming from the covalent bond formed between catechol group and organic surface.

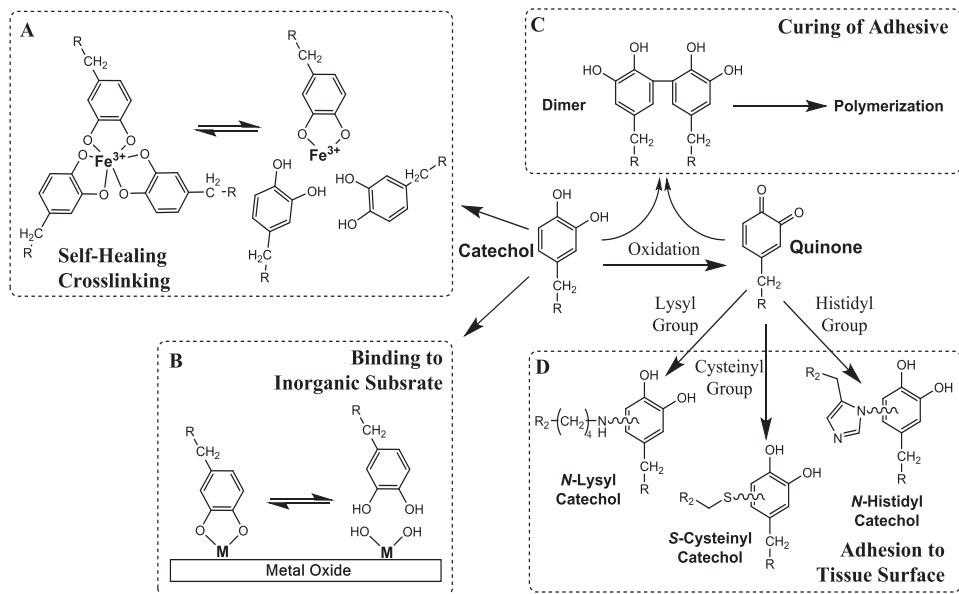


Figure 1-4. Schematic of catechol group reactions. A) catechol groups form reversible bond with metal ion; B) catechol groups react with metal oxide surface to form reversible bond; catechol groups oxidized into highly reactive quinones C) quinones react with each other to complete the polymerization; D) or react with different functional groups showing on the tissue surface to form covalent bond.

Recently, DOPA has been used to develop antifouling coatings<sup>[38-40]</sup> and tissue adhesives<sup>[41, 42]</sup>. A thermal-triggered gelation of DOPA-modified PEG hydrogel as bioadhesive was studied by Burke *et al.*<sup>[30]</sup> The oxidizing reagent was entrapped in liposome and released at body temperature. The hydrogel cured rapidly and showed a potential for biomedical application. Choi and coworkers<sup>[43]</sup> used tyrosinase to oxidize tyrosine residues in human gelatin into DOPA and they crosslinked the DOPA-modified gelatin into hydrogel by adding  $Fe^{3+}$  ions. Both of the results from *in vitro* and *in vivo* tests showed that DOPA- $Fe^{3+}$  gelatin hydrogel exhibited good mechanical properties and

hemostatic properties indicating that it is a promising tissue adhesive for surgical operations.

### 1.3 Poly(ethylene glycol)

Poly (ethylene glycol) is a polyether that can be easily synthesized into linear or branched (4-armed, 6-armed, 8-armed and superbranched) architecture with different molecular weights ranging from several hundred Da to ten million Da or more.<sup>[44]</sup> It is synthesized from ethylene oxide through anionic polymerization (Figure 1-5).

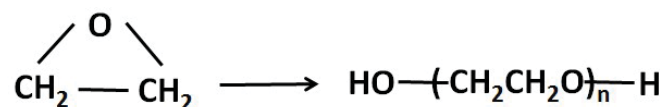


Figure 1-5. Synthesis of poly (ethylene glycol) from anionic polymerization of ethylene oxide.

PEG has been used in many biomedical applications because of its biocompatibility, non-immunogenicity and bioinert characteristics to resist cell or protein adsorption.<sup>[28, 45,</sup>

<sup>46]</sup> It is believed that when proteins are getting closed to the PEG-surface, the repulsive force is increased due to the decreased conformational freedom of the PEG chains. In addition, the osmotic interaction between proteins and PEG-surface due to the steric stabilization force will also repulse proteins from PEG-surface.<sup>[47]</sup> Vigilon<sup>TM</sup> and Hypol<sup>TM</sup> are two PEG-based commercial products. Vigilon<sup>TM</sup> is formed through the

radiation crosslinking of PEO and is used as wound cover material. Hypol<sup>TM</sup> is a PEG foam used in wound healing and drug delivery.<sup>[48]</sup> In recent years, PEG gel has also been investigated as vehicles for protein delivery<sup>[49]</sup> and three dimensional scaffolds<sup>[50]</sup>. However, the bioinert nature of PEG makes it lacking biological activity.

Inspired by nature, researchers modified PEG to mimic the natural extracellular matrix (ECM) and applied the modified PEG hydrogel in tissue engineering. RGD sequence is the most effective and widely used peptide sequence to stimulate cell adhesion of PEG.<sup>[51]</sup> RGD-mediated cell adhesion consists of four steps: cell attachment, cell spreading, organization of actin cytoskeleton and formation of focal adhesion. Integrin existing on the cell membrane binds with RGD ligand allowing cells to withstand shear force and anchor at a specific location. After the cell attachment, integrin-RGD ligand interaction is involved in the transmembrane signal transduction to regulate cell response, such as proliferation, differentiation and apoptosis. RGD peptide gradient was immobilized on the PEG scaffold to guide the cell migration.<sup>[52]</sup> Results revealed that cells tended to migrate in the direction of gradient with a higher speed than on the hydrogel with uniform distribution of RGD. PEG has also been modified with RGD peptide sequence to facilitate the cell adhesion and promote bone tissue regeneration.<sup>[53]</sup> There was a significant increase of mineralization after the introduction of RGD in the

network of hydrogel.

## 1.4 Gelatin

Gelatin is a soluble protein hydrolyzed from collagen.<sup>[54]</sup> Both collagen and gelatin were used in wound dressing and adhesives.<sup>[55]</sup> However, collagen expresses antigenicity in physiological condition while gelatin is known having no such antigenicity.<sup>[56, 57]</sup> The denature processes include the melting of ordered hydrogen bond and destroying of the triple helix structure to produce random chains of gelatin molecule. Since gelatin is obtained by hydrolyzing collagen which is the main component of ECM, it also contains RGD-like sequence to promote cell adhesion, migration and proliferation.<sup>[58]</sup> There are two types of gelatin: gelatin A, which is obtained by acidic pretreatment before denaturation; gelatin B, which is processed by alkaline pretreatment. The alkaline pretreatment leads to a higher content of carboxylic acid in gelatin B than that of gelatin A.<sup>[59]</sup> Molecular chains of gelatin undergo a coil-to-helix conformational transition to form physical thermo-reversible gels when the temperature of gelatin solution is lower than 35°C, in which process the gelatin molecules tend to recover the triple helix structure of collagen.<sup>[60, 61]</sup> However, the physical network of gelatin gel easily breaks down at a higher temperature. 1-ethyl-3-[3-dimethylaminopropyl]carbodiimide



hydrochloride (EDC) and N-hydroxysuccinimide (NHS) are widely used chemical crosslinking agent to improve the thermal and mechanical stability of gelatin gel.<sup>[13]</sup> Under reaction of EDC and NHS, -COOH groups and -NH<sub>2</sub> groups showing in the gelatin molecule will form covalent bonds<sup>[62, 63]</sup> (Figure 1-6).

A photocurable tissue adhesive glue composed of photoreactive gelatin and poly(ethylene glycol) diacrylate (PEGDA) was investigated by Nakayama *et al.*<sup>[64]</sup> Gelatin was modified with photoreactive groups and combined with PEGDA. Under exposure to the UV or visible light within 1min, water-swollen gels were produced and these gels showed a high adhesive strength to wet collagen film. When applied on the rat liver tissue, the gel tightly adhered to the native tissue through interpenetration and the gel stopped bleeding completely. Balakrishnan *et al.*<sup>[65]</sup> reported a self-crosslinked oxidized alginate/gelatin hydrogel as injectable biomimetic adhesive scaffold for cartilage regeneration. In their experiment the hydrogel was delivered with a minimally invasive injection and was cell-attractive. It functioned as an adhesive scaffold for the treatment of osteoarthritis. The hydrogel integrated well with cartilage tissue and showed a burst pressure of  $70 \pm 3$  mmHg, indicating the adhesive nature. Vandelli *et al.*<sup>[14]</sup> and Wu *et al.*<sup>[66]</sup> used crosslinked gelatin microgel as drug delivery vehicle. The gelatin microgel was synthesized via water/oil emulsion system and chemically

crosslinked. Drug molecule was loaded in the microparticle structure and released under the physiological environment. Results of subcutaneous injection showed that gelatin microgel exhibited good biocompatibility. Basic fibroblast growth factor incorporated gelatin microgel was investigated by Kawai and colleagues to accelerate tissue regeneration.<sup>[15]</sup> In the experiment the basic fibroblast growth factor incorporated gelatin microgel was added into artificial dermis and implanted into full-thickness skin defects on pig. The results showed that gelatin microgel impregnated with basic fibroblast growth factor accelerated the fibroblast proliferation and capillaries formation.

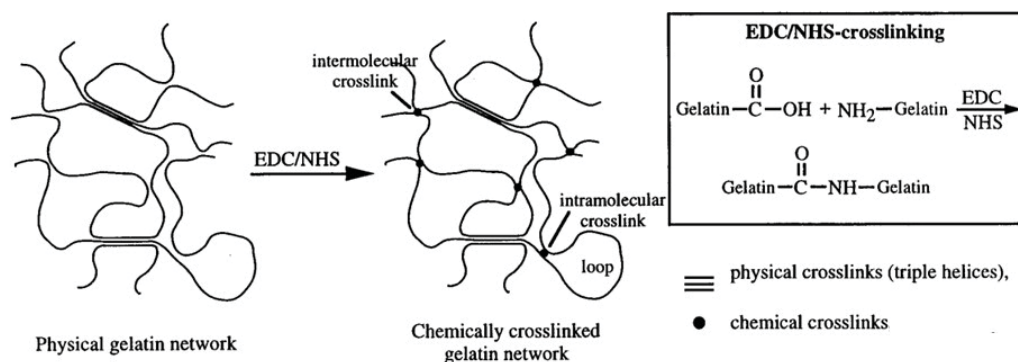


Figure 1-6. Schematic illustration of EDC/NHS involved chemical crosslinking.<sup>[62]</sup>  $-\text{COOH}$  and  $-\text{NH}_2$  groups in gelatin structure form covalent bond to chemically crosslink the gelatin hydrogel under the function of EDC and NHS. Reprinted with permission from [60]. Copyright (1999) American Chemical Society. (Copyright permission documentation in Appendix)

## 1.5 Wound healing

Wound healing is a complex process requiring interaction of different cells and tissues.<sup>[67]</sup> It consists of four steps: hemostasis, inflammation, proliferation, and remodeling and scar tissue formation.<sup>[68]</sup> The formation and contraction of newly formed connective tissue (granulation tissue) in step three is an essential step in wound healing to keep the tissue continuity.<sup>[69]</sup> During the normal wound healing, the inflammatory cells arrive to the wound bed first and followed by fibroblasts, which starts the deposition of collagen and other matrix component.<sup>[70]</sup> The newly formed connective tissue brings the edges of wound together through its contraction. Subsequently, a decrease in the cell number happens in the granulation tissue and the granulation tissue forms a poorly cellularized scar.<sup>[71]</sup> However, in many cases the cell apoptosis does not occur and there is no scar tissue formed. Then granulation tissue evolves into hypertrophic scar containing many myofibroblasts and inappropriately produced extracellular matrix, which results in a deformation of surrounding connective tissue. The deformation is considered as pathological issue. Therefore, it is very important to control the newly formed connective tissue to develop into a normal and functional tissue in the wound healing process.

## 2. Experimental

### 2.1 Materials

Gelatin powder (Type A, 300 Bloom, from porcine skin) was purchased from Electron Microscopy Sciences. Sodium periodate ( $\text{NaIO}_4$ , ACS reagent >99.8%), pyridine (ACS reagent, >99.0%), 1-ethyl-3-[3-dimethylaminopropyl]carbodiimide hydrochloride (EDC), N-hydroxysuccinimide (NHS), Masson's trichrome stain kit, bouin solution, Weiger's iron hematoxylin solution, TWEEN80 and glutaric anhydride were purchased from Sigma-Aldrich. Dulbecco's modified Eagle's medium (DMEM) was obtained from Corning Cellgro. Fetal bovine serum (FBS) was purchased from Thermo Scientific. Sodium pyruvate (100mM), MEM non-essential amino acid (100X) and 4-(2-hydroxyethyl)-1-piperazineethanesulfonic acid (HEPES) buffer solution (1M) were purchased from Life Technologies. 8-arm poly (ethylene glycol) (20K) was purchased from JenKem Technology. Dopamine hydrochloride was purchased from Acros Organics. O-(Benzotriazol-1-yl)-N,N,N',N'-tetramethyluroniumhexafluorophosphate (HBTU) and 1-hydroxybenzotriazole monohydrate (HOBt) were purchased from Chem-Impex International. Phosphate buffer saline and N,N-dimethylformamide (DMF) were purchased from Fisher Scientific. Chloroform was purchased from J.T

Baker.3-(4,5-dimethylthiazol-2-yl)-2,5-diphenyltetrazolium bromide (MTT) 98% was purchased from Alfa Aesar. 4',6-Diamidino-2-phenylindole (DAPI) was purchased from Invitrogen. Anti-S100A4 antibody (ab27957), goat anti-rabbit IgG H&L (Alexa Fluor 488; ab150077), anti-CD11b antibody (ab8879) and goat anti-mouse IgG (Alexa Fluor 488) (ab150113) were purchased from Abcam. Anti-CD163 antibody (sc-58965) and goat anti-mouse IgG (sc-2781) were purchased from Santa Cruz Biotechnology. Rat dermal fibroblast was isolated from rat dermal tissue and identified with Anti-S100A4 antibody and goat anti-rabbit IgG H&L (Alexa Fluor 488).<sup>[72]</sup> 12-well cell suspension culture plate was purchased from VWR International. Mechanical sieves were purchased from ATM Corporation. Dialysis tubing was purchased from Spectrum Labs (MWCO 3500).

## **2.2 Methods**

### **2.2.1 Synthesis of dopamine-modified 8-arm PEG (PEGDM)**

A two-step method was used to synthesize biodegradable dopamine-modified 8-arm PEG. The first step was to link glutaric acid to the end of PEG structure. 32g of 8-arm PEG powder was combined with 7.30g glutaric anhydride in a round bottom flask and

dissolved in 300mL chloroform and 5.16mL pyridine under nitrogen. The solution was refluxed under nitrogen for 24h. After which, most of the solvent was removed by rotary evaporation followed by the complete removal of the solvent in the vacuum system. The polymer was further dialyzed for 48h (pH around 3.0) to remove the unreacted molecules. The sample was then freeze-dried and characterized with nuclear magnetic resonance (NMR). The coupling efficiency was 81%, which was determined using NMR. The yield of product was 30g.  $^1\text{H}$  NMR (400MHz,  $\text{D}_2\text{O}$ )  $\delta$  3.75-3.39 (m, PEG), 2.37 (t, 2H,  $-\text{C}(=\text{O})-(\text{CH}_2)_2-\text{CH}_2-\text{C}(=\text{O})-$ ), 2.32 (t, 2H,  $-\text{C}(=\text{O})-(\text{CH}_2)_2-\text{CH}_2-\text{C}(=\text{O})-$ ), 1.79 (t, 2H,  $-\text{C}(=\text{O})-(\text{CH}_2)_2-\text{CH}_2-\text{C}(=\text{O})-$ ). (Figure A1 in Appendix)

To add dopamine molecule on the structure of PEG-glutaric acid (PEGGlu), 30g PEGGlu sample was combined with 5.45g dopamine HCl, 3.70g HOBt and 9.16g HBTU. The mixture was dissolved in 120mL of chloroform, 60mL of DMF and 4.01mL of triethylamine. After reacting for 3h the solution was rotary evaporated and completely dried in vacuum. Dialysis was performed for 48h (pH around 3.0) to remove the unreacted small molecules. The freeze-dried sample was characterized with NMR. The coupling efficiency was 80% which was determined using NMR. The yield of the product was 27.58g.  $^1\text{H}$  NMR (400MHz,  $\text{D}_2\text{O}$ )  $\delta$  6.71 (d, 1H,  $-\text{C}_6\text{H}_2\text{H}(\text{OH})_2$ ), 6.64 (d, 1H,  $-\text{C}_6\text{H}_2\text{H}(\text{OH})_2$ ), 6.56 (d, 1H,  $-\text{C}_6\text{H}_2\text{H}(\text{OH})_2$ ), 3.74-3.38 (m, PEG), 2.12 (t, 2H,

-C(=O)-(CH<sub>2</sub>)<sub>2</sub>-CH<sub>2</sub>-C(=O)-), 2.07 (t, 2H, -C(=O)-(CH<sub>2</sub>)<sub>2</sub>-CH<sub>2</sub>-C(=O)-), 1.67 (t, 2H, -C(=O)-(CH<sub>2</sub>)<sub>2</sub>-CH<sub>2</sub>-C(=O)-).(Figure A2 in Appendix)

### 2.2.2 Preparation of gelatin microgel

2g of gelatin powder was dissolved in 20mL of deionized water (DI water) in 50-55°C water bath. The solution was stirred with magnetic stir bar in water bath at 50-55°C for 10min. The gelatin solution was added dropwise into 200mL preheated olive oil under stirring at 1000 rpm in 50-55°C water bath for 1h to form an emulsion. The temperature of the emulsion was lowered to room temperature and the emulsion was kept stirring for 30min. In order to continue solidifying the gelatin microgel, the container of reaction system was placed in ice water bath for 30min to lower the temperature. 100mL precooled acetone (4°C) was added into the emulsion mixture to wash the microgel for 30min in ice water bath. The overhead stirrer kept stirring until the end of wash step. The microgel was separated from olive oil and acetone through vacuum filtration. The separated microgel was washed twice in 60mL precooled acetone. The size distribution was controlled in the range of 53-75µm using the mechanical sieves and the microgel was stored at 4°C. The yield of produced microgel was  $0.72 \pm 0.05$ g.

In order to chemically crosslink the gelatin microgel, 0.5g of microgel was suspended in 30mL of phosphate buffer saline (PBS) (pH=5.7, 0.5% TWEEN 80). 0.134g of EDC and 0.02g of NHS were added into the microgel suspension to start the crosslink reaction. The reaction mixture was kept at 4°C for 24h. After which, the microgel was washed twice with 60mL of precooled (4°C) acetone to remove EDC and NHS and the reaction was stopped. The Crosslinked microgel was collected with vacuum filtration and the dry product was stored at 4°C. The yield of the crosslinked microgel was  $0.43 \pm 0.02$ g. The morphology of gelatin microgel was characterized with scanning electron microscope (SEM).

### **2.2.3 Preparation and characterization of gelatin microgel incorporated PEG (PEG-GM) adhesive**

Gelatin microgel was suspended in polymer precursor solution containing PEGDM (30wt% PEGDM and 0-15wt% gelatin microgel) in 10mM PBS buffered at pH 7.4. The PEG-GM adhesive was prepared by mixing equal volumes of PEGDM/microgel mixture and NaIO<sub>4</sub> solution (11.67mg/mL in DI water). The molar ratio of NaIO<sub>4</sub> and dopamine was 0.5 and the final concentrations of PEGDM and gelatin microgel were 15wt% and 0-7.5wt%, respectively. The cure time was determined when the mixture



stopped to flow in a tilt vial (Figure 2-1).<sup>[73]</sup> The adhesives used in the following experiments were allowed to cure for 12h and were cut into dish shape. The dish-shaped adhesives were equilibrated in PBS (pH 7.4) for the following tests.



Figure 2-1. Image of the experiment to determine the cure time of adhesive. The cure time was determined when the adhesive solution stopped flow in a tilt vial. 8

Adhesive samples with (7.5wt%) and without (0wt%) gelatin microgels were vacuum-dried for 2 days. Fourier transform infrared spectroscopy (FTIR) was performed using a PerKinElmer Spectrum One Spectrometer to obtain the FTIR spectra of dry samples.

Adhesive samples (n=4) with 0wt%, 1.5wt%, 3.75wt% and 7.5wt% gelatin microgel were equilibrated in PBS (pH=7.4) at room temperature overnight. The mass of swollen

samples ( $M_s$ ) were weighed after the equilibration. Samples were then vacuum-dried for 2 days to obtain the dry mass of adhesives ( $M_d$ ). The equilibrium water content (EWC) was determined by equation of:

$$\text{EWC} = (M_s - M_d) / M_s \times 100\% \quad (\text{Equation 1})$$

## **2.2.4 Mechanical properties**

### **2.2.4.1 Compression test**

6 pieces of adhesive disc samples of each formulation (0wt%, 1.5wt%, 3.75wt% and 7.5wt%) were tested. The dimensions of the samples were ~3mm in thickness and ~7mm in diameter, measured individually with a digital caliper. The samples were compressed using Bose ElectroForce mechanical testing machine at a rate of 0.03mm/second until the adhesive structure completely fractured. The stress was calculated by dividing the load measured by the surface area of the sample. The strain was obtained by dividing the place changes of compression plate by the original thickness of the sample. The failure stress and failure strain were determined when the first fracture occurred. Toughness was determined by the integration of the area under

the stress-strain curve. The elastic modulus was determined based on the slope of the stress-strain curve at a strain between 0.05 and 0.12.

#### **2.2.4.2 Oscillatory rheometry**

The storage ( $G'$ ) and loss ( $G''$ ) modulus was determined under frequency of 0.1-100 Hz at strain of 0.1 using a rheometer (HR-2, TA Instruments, New Castle, DE). Adhesive discs (diameter= 8 mm, thickness = 1 mm, n = 3) were tested using parallel plates at a gap distance that is set at 85% that of the individual adhesive thickness, as measured by a digital vernier caliper.

#### **2.2.5 Lap shear test**

Adhesive property of PEG-GM adhesive was tested according to the American Society for Testing and Materials (ASTM) standard F2255-05. 60 $\mu$ L of PEG polymer precursor solution and 60 $\mu$ L of NaIO<sub>4</sub> solution were added onto the overlap area of two pieces of bovine pericardium and cured *in situ* with an overlap area of 2.5cm x 1cm. A 100g weight was immediately loaded on the top of overlapping area for 10min (Figure 2-2). After the complete gelation, samples were placed in the PBS solution and incubated at

37°C overnight. The adhesive area of each sample was measured in both length and width before the testing with a digital caliper. The samples were pulled at a rate of 5mm/min until completely separated. The adhesive strength and the work of adhesion were obtained respectively by dividing the max load and the integral of the area under the load-displacement curve by the adhesive area measured before the test.<sup>[74]</sup>

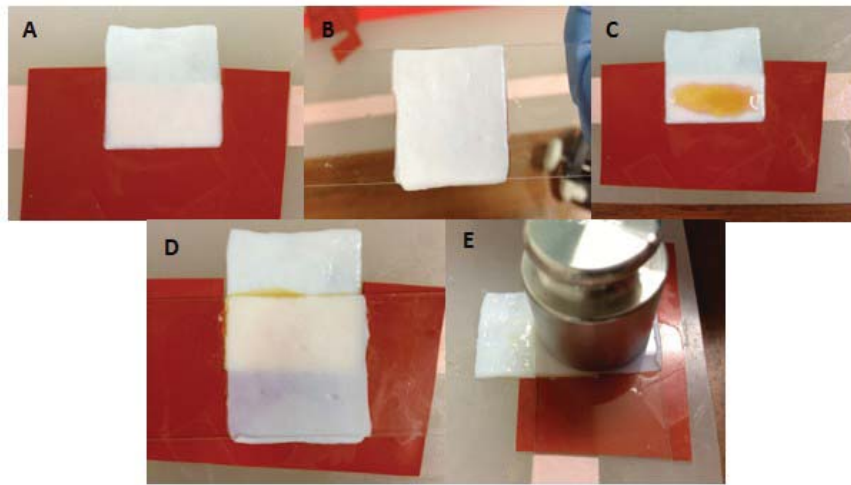


Figure 2-2. Photographs of preparation for lap shear test. A) One piece of bovine pericardium placed in a mold; B) the other piece of bovine pericardium placed on a glass slide; C) adhesive precursor solutions was mixed in the overlap area; D) the mixed precursor solution covered by the other piece of bovine pericardium; E) 100g weigh loaded on the overlap area for 10min.

### 2.2.6 *In vitro* degradation test

PEG-GM adhesives containing 0wt%, 1.5wt%, 3.75wt% and 7.5wt% gelatin microgel were punched into disc shape (thickness=1mm, diameter=8mm) and incubated in 2mL PBS at 37°C. PBS was changed every 7 days. Three pieces of adhesive were dried in

each formulation group and recorded the dry weight of adhesive.  $M_0$  is the average dry weight of adhesive at original status. Three repeat samples in each formulation group were then collected every week and dried to weigh the weight of adhesive to determine the remaining mass after degradation,  $M_t$ . The degradation was determined by:

$$\text{Degradation\%} = M_t / M_0 \times 100\% \quad (\text{Equation 2})$$

## **2.2.7 Cell experiment**

### **2.2.7.1 Cell viability**

In order to evaluate the cytotoxicity of PEG-GM adhesive, quantitative MTT cytotoxicity assay according to the ISO 10993-5 guideline was conducted. L929 mouse fibroblast was cultured in culture medium containing 10% FBS and 10 units/mL penicillin-streptomycin in DMEM at 37°C. Adhesive extract was obtained by incubating the adhesive discs in the culture medium for 24h and using 0.22 $\mu$ m sterile filters to sterilize the adhesive extract<sup>[75]</sup>. Meanwhile, cells were seeded into 96-well culture plate at the density of  $1 \times 10^4$  cell/cm<sup>2</sup>. Each well was then added 100 $\mu$ L of culture medium and incubated for 24h to obtain a confluent monolayer of cells. After 24h the cell culture

medium was removed and 100 $\mu$ L adhesive extract was added into each well. The adhesive extract was then replaced by 50 $\mu$ L MTT solution (1mg/mL in PBS) after 24h incubation and continued to incubate for another 2h. 100 $\mu$ L DMSO was added into each well to replace the MTT solution. The absorbance was measured at 570nm with a Synergy HT Multi-Mode Microplate Reader (BioTek, USA). Three tests were repeated for each formulation group. The relative cell viability was calculated with:

$$\text{Cell viability\%} = A_{\text{adhesive}}/A_{\text{control}} \times 100\% \quad (\text{Equation 3})$$

Where  $A_{\text{adhesive}}$  is the absorbance for cells cultured in adhesive extract and  $A_{\text{control}}$  is the absorbance for cells cultured in cell culture medium. The test was repeated for three times for each formulation (0wt%, 3.75wt% and 7.5wt%). Samples were considered non-cytotoxic when they had a relative cell viability higher than 70%.<sup>[75]</sup>

### **2.2.7.2 Cell attachment**

PEG-GM adhesives containing 0wt%, 3.75wt% and 7.5wt% gelatin microgel were punched into dish shape (thickness=0.5mm, diameter=10mm). Adhesive samples were sterilized with 70% ethanol for 45min and balanced with PBS for three times, each time

lasting 30 min.<sup>[75]</sup> Rat dermal fibroblasts with a density of  $3.2 \times 10^4$  cell/cm<sup>2</sup> were seeded on the surface of adhesive samples in a 12-well cell suspension culture plate. The cells were seeded on the surface of adhesive for 30 min in an incubator and subsequently cultured for another 72 h at 37°C. Cell density was quantified using ImageJ software after the DAPI staining. Calcine and ethidium bromide were diluted in PBS at 1: 1000 ratio. Cells were incubated in the calcine/ethidium bromide solution for 3 min. The cell morphology was observed by calcine staining. The calcine-stained cells were considered as living cells which have been successfully attached on the adhesive and continue to proliferate.<sup>[76]</sup> Ethidium bromide-stained cells were considered as dead cells.

### **2.2.8 Subcutaneous implantation**

Healthy, weight matched Sprague Dawley rats were provided by Michigan Technological University animal care facility. The subcutaneous implantation was performed following the protocol approved by Michigan Technological University Institutional Animal Care and Use Committee. Disc-shaped PEG-GM adhesives containing 0 wt% and 7.5 wt% gelatin microgel (diameter=10 mm and thickness=1.5 mm) were subcutaneously implanted. Each formulation has four pieces of repeat sample. Samples were sterilized using ethanol-based sterilization method (samples were soaked

in 20mL 70% ethanol for 45min and washed with 20mL PBS for 30min for three times<sup>[75]</sup>) Rats were anesthetized with isoflurane-oxygen gas. Fur in the surgical area was removed and surgical sites were sterilized with ethanol and betadine. Four bilateral pouches were formed with sterile surgical scissors on the back of rats. Samples were implanted into the pouches. Wounds were closed with surgical staples. After 2 weeks and 6weeks recovery, rats were sacrificed. Samples and surrounding tissue were collected and flash frozen in Polyfreeze for the following cryosection. Samples were sectioned into 10 $\mu$ m thick sections and stained with Hematoxylin and eosin (H&E) staining and Masson's trichrome staining to evaluate the morphology and collagen formation, respectively. Fibroblast marker S100A4, M1 macrophage marker CD11b and M2 macrophage marker CD163 were used for immunohistochemistry staining to analyze the inflammatory response and wound healing process.<sup>[75, 77, 78]</sup> All images were taken with Olympus microscope and analyzed with ImageJ software.

### **2.2.9 Statistical analysis**

Statistical analysis was performed using SigmaPlot software. Student t-test and one-way analysis of variance (ANOVA) were used to compare the means of two groups and multiple groups, respectively. A statistical difference was determined when *p*-value was



less than 0.05.

### **3. Results and discussions**

#### **3.1 Preparation and characterization of materials**

Gelatin microgel was synthesized via water in oil emulsification method.<sup>[14]</sup> The surface morphology of harvest gelatin microgel was characterized using SEM (Figure 3-1) and the average diameter of gelatin microgel was  $53.57 \pm 14.23 \mu\text{m}$ .

Gelatin microgel incorporated PEG adhesive was prepared with a simple operation under mild condition. Microgels were suspended into PEG precursor solution at room temperature first. Then the gelatin microgel containing PEG precursor solution and the  $\text{NaIO}_4$  solution were fully mixed at room temperature and gelled in a minute. The cure time of PEG-GM adhesive decreased with increasing weight percentage of gelatin microgel (Figure 3-2). The average cure time of 0wt% PEG-GM adhesive was 54 second and the cure time decreased gradually with increasing weight percentage of gelatin microgel. The 7.5wt% PEG-GM adhesive exhibited the shortest gelation time (37 seconds). PEGDM adhesive cures through the polymerization of catechol groups in

the dopamine structure with the introduction of the chemical oxidant ( $\text{NaIO}_4$ ).<sup>[73, 79]</sup> Additionally, quinones which are oxidized from catechol groups can form covalent bond with  $-\text{NH}_2$  found on the gelatin microgel surface.<sup>[36]</sup> As such, the number of cohesive chemical crosslinks needed for network formation was reduced with increasing microgel content, and resulted in a reduced cure time. A similar result was reported by Liu *et al.*<sup>[75]</sup> that the incorporation of nanoparticles decreased the gelation time of dopamine-modified PEG adhesive.

For comparison purposes, we attempted to incorporate gelatin polymers into PEGDM adhesive by directly blending it into the precursor solution. However, at the concentrations that were tested in this study, gelatin was not soluble in the precursor solution at room temperature. In order to dissolve gelatin, the temperature of the precursor solution needed to be raised to above  $50^\circ\text{C}$ , but the mixture solidified upon cooling as a result of physical bond formation within the gelatin polymer chains. This temperature dependent curing of gelatin made it not possible to create an *in situ* curable adhesive through direct blending of gelatin polymer.

Fourier transform infrared spectroscopy (FTIR) was used to confirm the incorporation of gelatin microgel into PEGDM adhesive (Figure 3-3). FTIR spectrum contains peaks

for ether bond ( $1000-1150\text{ cm}^{-1}$ ), ester bond ( $1731\text{ cm}^{-1}$ ), phenols ( $3200-3500\text{ cm}^{-1}$ ) and aromatics ( $1400-1500\text{ cm}^{-1}$ ) of PEGDM and amide bond peaks ( $1568$  and  $1640\text{cm}^{-1}$ ) of PEGDM and PEG-GM. The intensity of amide bond peak increased with the incorporation of gelatin microgel while the intensity of ester bond remained unchanged, confirming the incorporation of gelatin microgel into PEG adhesive.

Equilibrium water content (EWC) was measured to determine the physical property of the adhesive network. The value of EWC is inversely proportional to the crosslink density of adhesive network.<sup>[80]</sup> As shown in the Figure 3-4 EWC decreased from  $90.1\% \pm 0.4\%$  to  $86.6\% \pm 0.5\%$  with increasing content of gelatin microgel, which indicated that the crosslink density of adhesives increased significantly with increasing content of gelatin microgel.

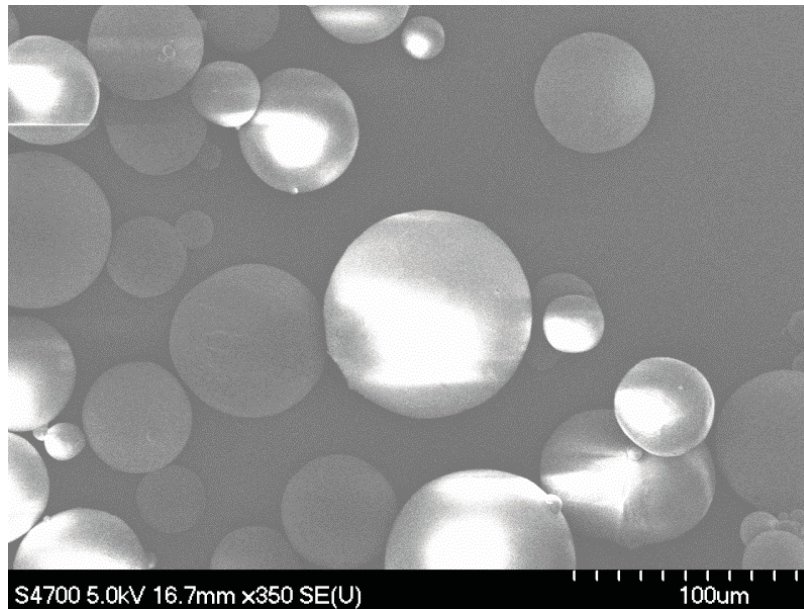


Figure 3-1. SEM image of gelatin microgel.

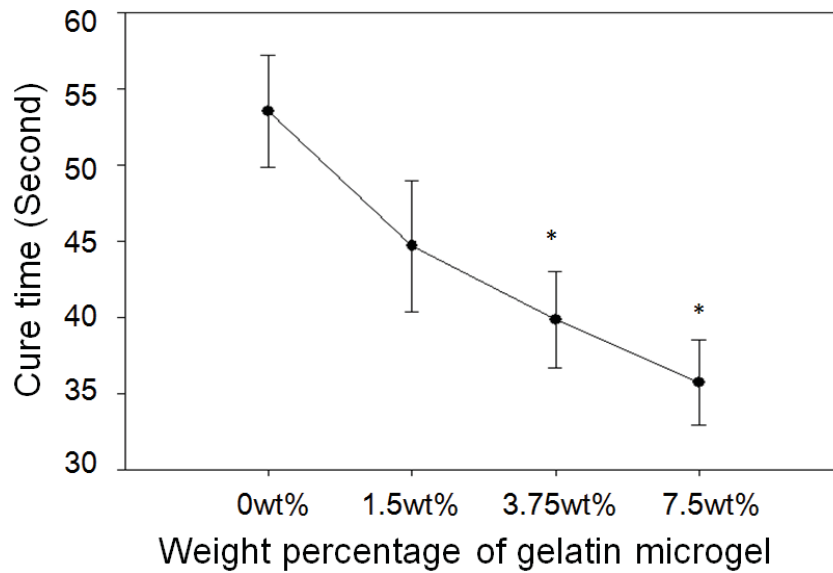


Figure 3-2. Cure time of PEG-GM adhesive with different gelatin microgel weight percentage. The cure time decreased with the increasing weight percentage of gelatin microgel. \*  $p < 0.05$  when compared with 0wt% adhesive.

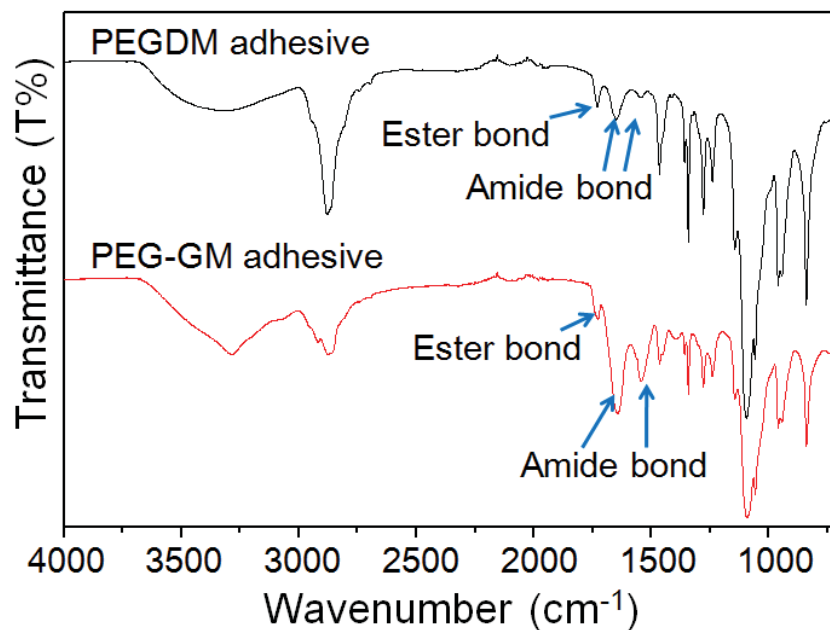


Figure 3-3. FTIR results of PEGDM adhesive (black) and PEG-GM adhesive (red).

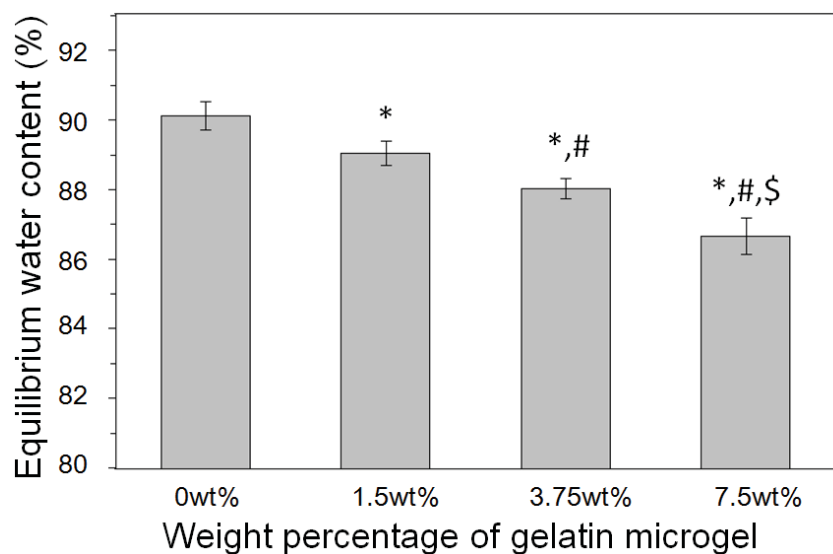


Figure 3-4. Equilibrium water content of PEG-GM adhesive with different gelatin microgel weight percentage. The equilibrium water content decreased with increasing weight percentage of gelatin microgel. \*  $p < 0.05$  when compared with 0wt% adhesive; #  $p < 0.05$  when compared with 1.5wt%

adhesive; \$ p < 0.05 when compared with 3.75wt% adhesive.

## 3.2 Mechanical property test

### 3.2.1 Compression test

From unconfined, uniaxial compression test, incorporation of gelatin microgel increased the elastic modulus of PEG-GM adhesive while other parameters such as the maximum strength, failure strain and toughness were unaffected (Table 3-1). The increase in the measured modulus corresponded with increased crosslinking density of PEG-GM, which corroborated with results from EWC. The increased crosslinking density led to a stiffer adhesive. However, the crosslinked bulk gelatin gel showed a significantly lower modulus compared to those of PEG-GM adhesives (Table A1 in Appendix). Since the failure strain showed no significant decrease with increasing content of gelatin microgel. Therefore, the compliance of adhesive was not compromised with the increased stiffness.

Table 3-1. Compression test results of 0wt%, 1.5wt%, 3.75wt% and 7.5wt% PEG-GM adhesive.

	0wt%	1.5wt%	3.75wt%	7.5wt%
Failure stress/kPa	407 ± 49.9	460 ± 37.8	450 ± 36.4	423 ± 28.4

Failure strain	0.64 ± 0.03	0.62 ± 0.02	0.60 ± 0.01	0.57 ± 0.03
Elastic modulus/kPa	151 ± 10.0	161 ± 5.1	177 ± 15.1*	204 ± 11.1*.#
Toughness/kJ/m <sup>3</sup>	183 ± 11.5	199 ± 8.2	193 ± 17.7	196 ± 37.7

\* p < 0.05 when compared with 0wt% adhesive; # p < 0.05 when compared to 1.5wt% and 3.75wt% adhesives

### 3.2.2 Oscillatory rheometry

The viscoelastic property of adhesive was determined through the oscillatory rheometry test. The storage modulus ( $G'$ ) was significantly higher than the loss modulus ( $G''$ ) in all groups (Figure 3-5), indicating that the adhesive were fully crosslinked. The  $G'$  of 0wt% sample (control group) was independent of frequency at a frequency less than 25Hz, which also indicated a chemically crosslinked network. On the other hand, there was a slightly increase in  $G'$  values with increasing frequency for microgel incorporated samples, which indicated the presence of reversible physical bonds in the adhesive network.<sup>[81]</sup>  $G'$  values increased sharply for all the samples tested at elevated frequencies (>25 Hz). This stiffening phenomenon is a typical behavior of chemically crosslinked network, associated with polymer chains not having sufficient time to relax.<sup>[82]</sup>

The increased  $G'$  with the increasing content of gelatin microgel indicates a higher

crosslink density due to the presence of gelatin microgel. The catechol groups showing in the PEG adhesive structure reacted with gelatin microgel and formed chemically crosslinking. This matches the increased elastic modulus in compression test. Both of these two results indicate a stiffer material with a higher content of gelatin microgel.

$G''$  values also increased with the increasing content of gelatin microgel. Most noticeably, the adhesive containing 7.5wt% microgel exhibited a  $G''$  value that was over an order of magnitude higher than those of formulations containing 0wt% and 1.5wt% microgel. The elevated  $G''$  revealed an increased viscous dissipation ability of adhesive.<sup>[83]</sup> Molecular chains of gelatin undergo a coil-to-helix conformational transition to form physical thermo-reversible gels at a lower temperature ( $< 35^{\circ}\text{C}$ ), in which process the gelatin molecules tend to recover the triple helix structure of collagen.<sup>[60, 61]</sup> The reversible physical bonds existing in the gelatin microgel and the hydrogen bond in the adhesive network can be sacrificed before the breaking of chemical bond during the energy dissipation.



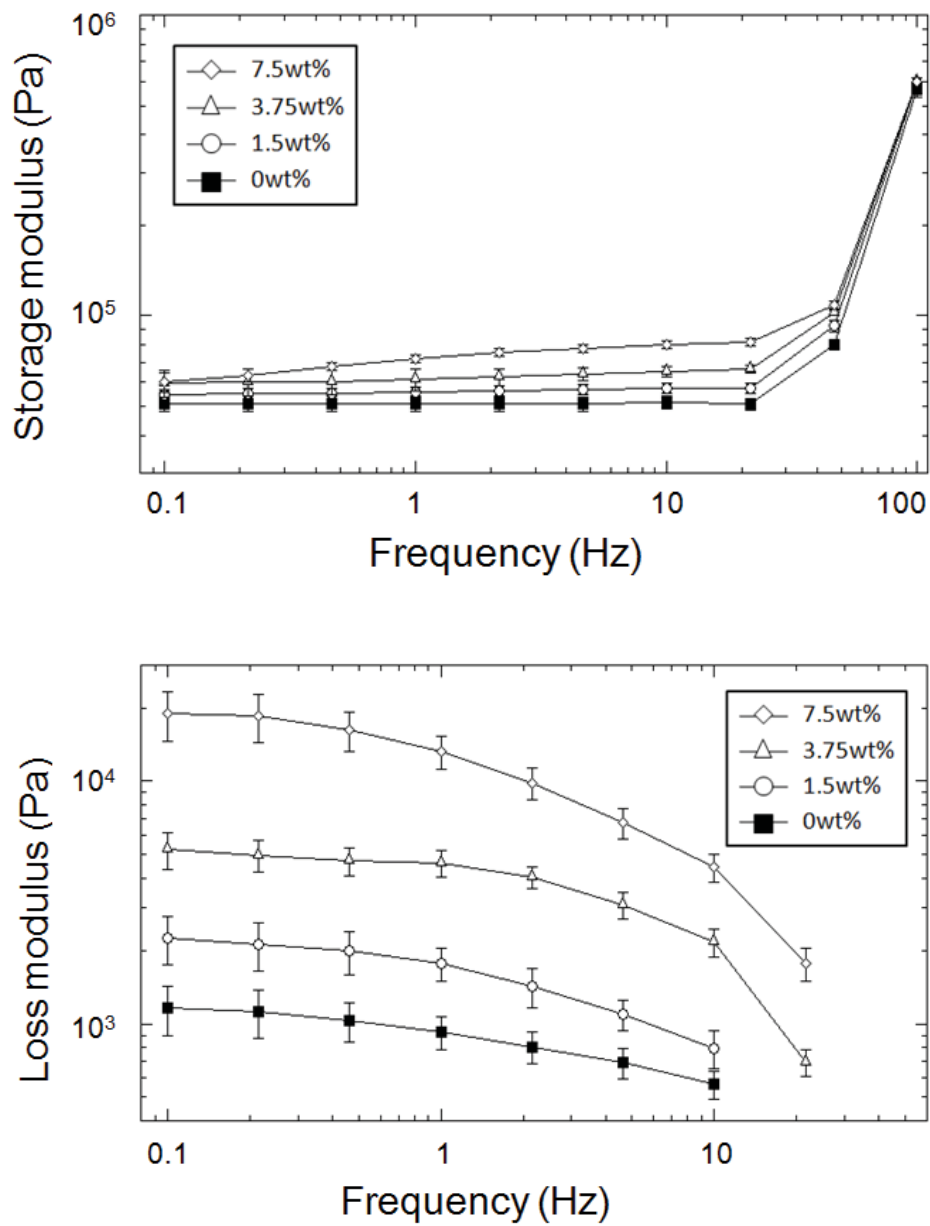


Figure 3-5. Storage and loss modulus of PEG-GM adhesive. The storage modulus and loss modulus increased with the increasing weight percentage of gelatin microgel.

### 3.3 Lap shear test

As shown in the figure 3-6, the adhesive strength and the work of adhesion of PEG-GM

adhesives were significantly higher (1.5-2 folds) than the control group (0wt%). The increased work of adhesion was attributed to the reversible physical bonds in the adhesive structure, such as the physical bond existing in the gelatin microgel structure. PEG-GM adhesive presented 2-fold higher work of adhesion due to the existence of gelatin microgel compared with the dopamine-modified PEG hydrogel incorporated with inorganic nanoparticle<sup>[75]</sup>. But the adhesive property reported here is weaker than those in other studies of catechol-modified PEG systems.<sup>[30, 78]</sup> It is difficult to compare this result with those in other studies due to the usage of different tissue and the testing protocols (different methods used to prepare testing samples, strain rate, etc.).

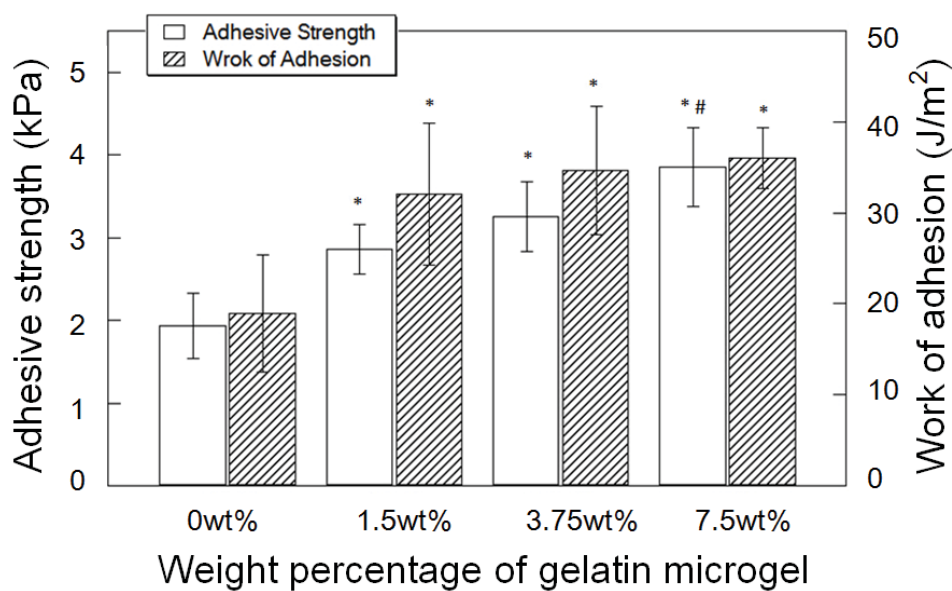


Figure 3-6. Lap shear adhesion test results of PEG-GM adhesive with different weight percentage of gelatin microgel. \*  $p < 0.05$  when compared to 0wt% adhesive. #  $p < 0.05$  when compared to 1.5wt% adhesive.

### 3.4 *In vitro* degradation test

In the *in vitro* degradation test, adhesives with different weight percentage of gelatin microgel degraded at a similar rate (Figure 3-7). The degradation went slowly in the first 6 weeks and all the gels lost their 70% mass after 8 weeks. After 8 weeks all the adhesives were completely degraded. There is no significant difference between different testing groups, indicating that degradation occurred mainly through the hydrolysis of the ester bond between the PEG and glutaric acid. The fast degradation after 8 weeks was attributed to the loose structure of adhesive and more water molecule penetrated into the adhesive structure to complete the degradation.

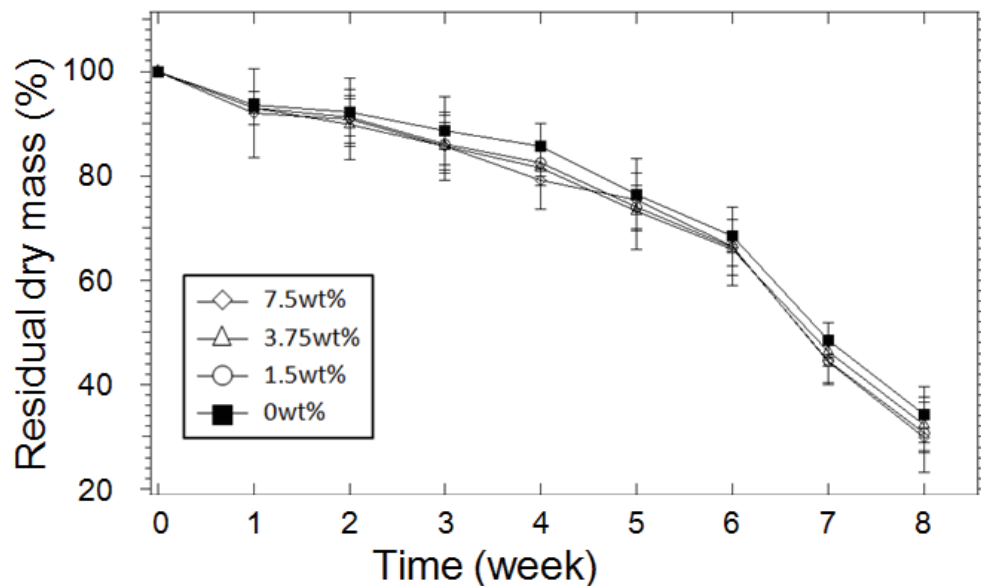


Figure 3-7. *In vitro* degradation test of PEG-GM adhesives containing 0wt%, 1.5wt%, 3.75wt% and 7.5wt% gelatin microgels.

## **3.5 Cell experiment**

### **3.5.1 Cell viability**

MTT assay was performed to evaluate the cytotoxicity of PEG-GM adhesives (0wt%, 3.75wt% and 7.5wt%). The relative cell viability showed no significant difference between the control group (0wt%) and test groups (3.75wt% and 7.5wt%) (Figure 3-8). All the results of the three groups were higher than 70% which is considered as biocompatible and noncytotoxic. The catechol modified PEG hydrogels previously studied either in our lab or other investigators all presented as biocompatible and noncytotoxic.<sup>[75, 78, 79, 84]</sup> Additionally, gelatin is biocompatible and its degradation product is also nontoxic.<sup>[14]</sup> Therefore it can be concluded that PEG-GM adhesive was noncytotoxic.

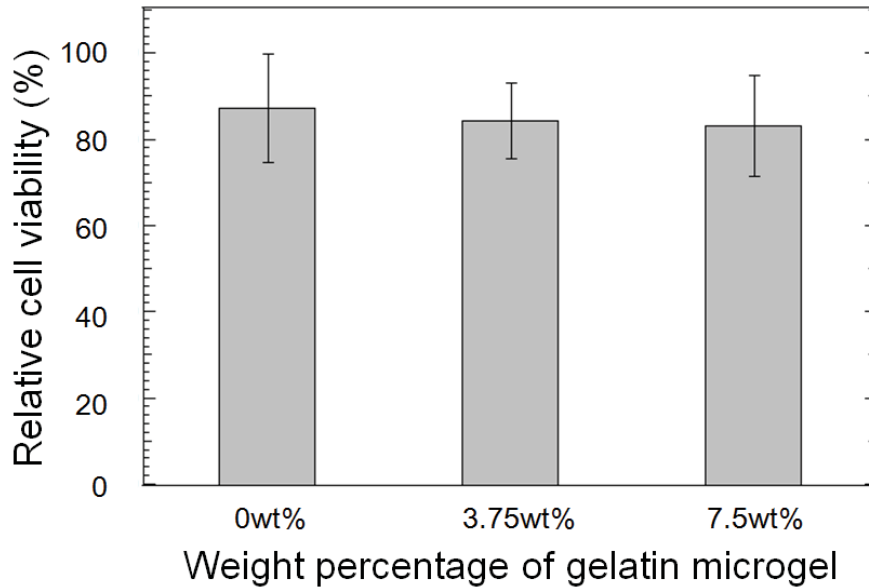


Figure 3-8. Relative cell viability test results of PEG-GM adhesives containing 0wt%, 3.75wt% and 7.5wt% gelatin microgel.

### 3.5.2 Cell attachment

Primary rat dermal fibroblasts were seeded on the surface of PEG-GM adhesive and the cellular density of the attached cells was quantified after DAPI staining (Figure A3 in Appendix). The cell number increased significantly with increasing weight percentage of gelatin microgel. The number of attached cell on the 7.5wt% was about 4-fold higher than control group (0wt%) and 2-fold higher than 3.75wt% group (Figure 3-9). Calcine and ethidium bromide were used to stain living (green) and dead (red) cells, respectively (Figure 3-10). The live/dead staining results showed that the ratio of living and dead

cells was  $1 \pm 0.25/3 \pm 0.47$  on the 0wt% group and the living cells appeared rounded in shape indicating that these cells were not attached well (Figure 3-10A)<sup>[76]</sup>. More cells attached and spread on the 3.75wt% adhesive, although there were some cells in rounded shape (Figure 3-10B). Most cells on the 7.5wt% adhesive were spread well (Figure 3-10C). No dead cells were found on the 3.75wt% and 7.5wt% adhesives. Gelatin microgels were also stained green through non-specific binding (blue arrows in Figure 3-10 B and C), and there is evidence for co-localization of the attached cells and the underlying gelatin microgels (Figure 3-10 B and C). The figures of DAPI staining (Figure A3 in Appendix) also support the co-localization of attached cells and gelatin microgels.

All the results discussed above indicated that the incorporation of gelatin microgel promoted cells attachment and spreading, both of which are essential for the cell survival and proliferation.<sup>[85-87]</sup> The gelatin microgel provided cell binding sites (i.e., RGD peptide sequences)<sup>[51, 53]</sup> and increased gelatin microgel content promoted cell attachment and spreading. Additionally, as reported by Discher *et al.*<sup>[88]</sup> and Yeung *et al.*<sup>[89]</sup> fibroblasts tend to spread on a stiffer substrate. This can also explain the difference among these three testing groups.

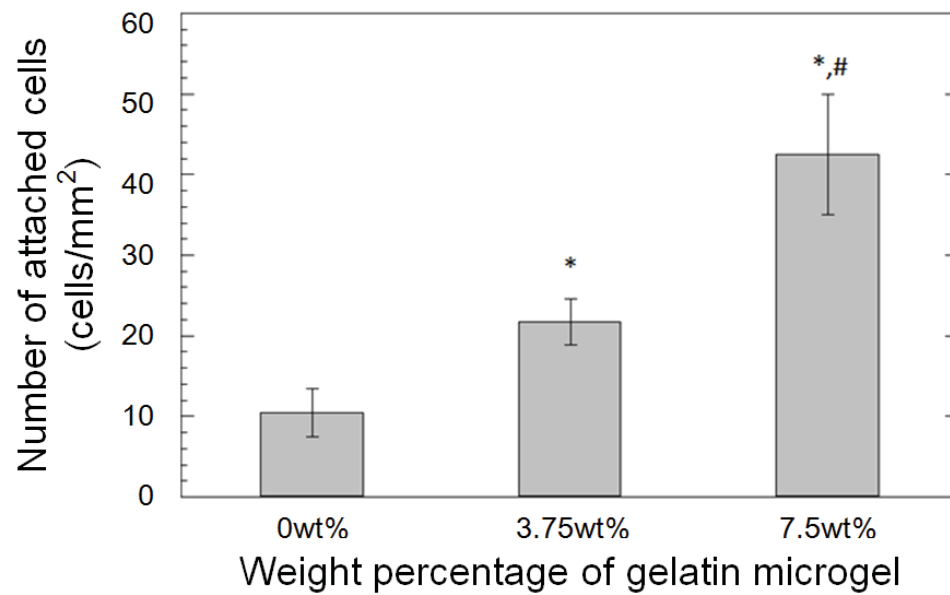


Figure 3-9. Cell attachment result. The number of attached rat dermal fibroblasts on the adhesive increased with the increased weight percentage of gelatin microgel. \*  $p < 0.05$  when compared to 0wt% adhesive. #  $p < 0.05$  when compared to 3.75wt% adhesive.

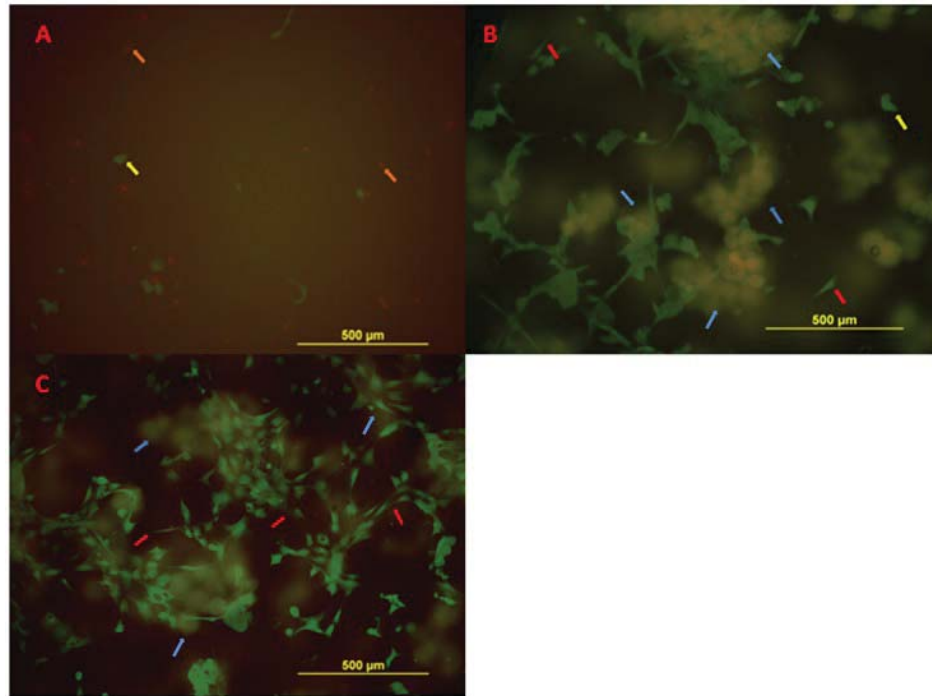


Figure 3-10. Live/dead staining result of cell attachment test. Cells spread better with increasing weight percentage of gelatin microgel. A: 0wt% adhesive; B: 3.75wt% adhesive; C: 7.5wt% adhesive. Living cells were stained in green and dead cells were stained in red. Gelatin microgels were also stained into green through non-specific binding. Blue arrow: gelatin microgel; Red arrow: spread cells; Orange arrow: dead cells; Yellow arrow: Living cells but not spread.

### 3.6 Subcutaneous implantation

PEG-GM adhesives with 0wt% and 7.5wt% gelatin microgel were subcutaneously implanted into rats for 2 and 6 weeks to evaluate the *in vivo* biocompatibility and bioactivity of the adhesive. The H&E and Trichrome staining revealed that after 2 weeks of implantation, more cells were present near the tissue-adhesive interface of 7.5wt% adhesive ( $7.7 \pm 0.9$  cells/mm<sup>2</sup>) than 0wt% adhesive ( $5.3 \pm 0.8$  cells/mm<sup>2</sup>) (Table 3-2 and



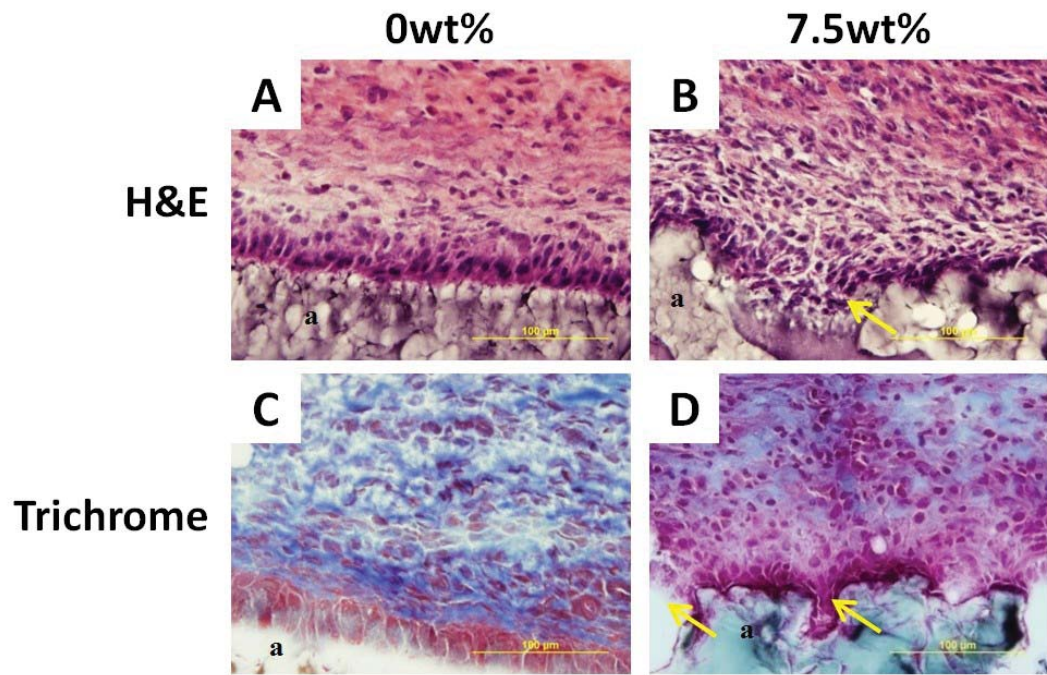
Figure 3-11 A-D). Through the immunofluorescent staining M1 macrophage and fibroblast were observed in the tissue-adhesive interface (Figure 3-11 E and F, I and J), while M2 cells were found further away from the tissue-adhesive interface (Figure 3-11 G and H). The results of 6 weeks of implantation showed higher cell density in tissue-adhesive interface of 7.5wt% adhesive ( $3.4\pm 0.64$  cells/mm<sup>2</sup>) than that of 0wt% adhesive ( $2.02\pm 0.66$  cells/mm<sup>2</sup>) (Figure 3-12 A and B). However, when compared to the 2 weeks test result, the cell density of 6 weeks test was obviously lower (Table 3-2). The thickness of collagen deposition around 7.5wt% adhesive ( $74.31\pm 14.14$   $\mu$ m) was also higher than that surrounding the 0wt% adhesive ( $43.63\pm 14.4$   $\mu$ m) after 6 weeks of implantation (Figure 3-12 C and D). Fibroblast and macrophage were observed in the same area as the result of 2 weeks implantation (Figure 3-12 E-J). Cell infiltration into the pocket structure via the degradation of previously contained gelatin microgel (single headed arrows in Figure 3-11 and 3-12) was observed at both time points. However, the pocket structure after 6 weeks of implantation is not as clear and regular as that of 2 weeks implantation due to the degradation of surrounding PEGDM adhesive. The degradation of PEGDM adhesive resulted in an irregular and uneven tissue-adhesive interface. Additionally, no cell infiltration into the pocket structure was observed in the results of 2 weeks and 6 weeks implantation of control groups (0wt%). There was no significant difference on the average infiltration layer thickness between control group

and 7.5wt% group after 6 weeks of implantation (Table 3-2).

M1 macrophage was the predominant cell type found in the tissue-adhesive interface area in both 2 weeks and 6 weeks test for 0wt% and 7.5wt% adhesives, indicating an inflammatory response due to the degradation of materials.<sup>[4, 90]</sup> The degradation of both PEGDM and gelatin microgel will lead to an uneven surface which will subsequently induce inflammatory response surrounding the implanted materials. The higher cell density in the interface of gelatin microgel containing adhesives is due to the activation of macrophage by gelatin.<sup>[91, 92]</sup> Fibroblasts were then attracted by the macrophage and started the deposition of collagen molecule.<sup>[93]</sup> The higher deposition of collagen molecule surrounding the 7.5wt% adhesive after 6 weeks can be potentially used in the wound healing of connective tissue. However, in order to achieve a successful and normal wound healing process of connective tissue we need to further control the collagen matrix formation into a normal and functional tissue.<sup>[70, 71]</sup> The presence of M2 macrophage indicated a wound healing process.<sup>[94]</sup>

Based on the discussion above, although there was M1 macrophage existing around the adhesives, the cell density was significantly reduced after 6 weeks implantation compared to 2 weeks implantation, indicating a reduced inflammatory response. The

deposition of collagen and the existence of M2 macrophage are signs of wound healing.<sup>[68, 94-97]</sup> Therefore, the PEG-GM adhesive can be considered as biocompatible.<sup>[98]</sup> The cell infiltration into the pocket structure via the degradation of gelatin microgel was observed in both 2 weeks and 6 weeks tests, indicating that gelatin microgel can be degraded by cells and it can provide space for cell infiltration. However, there was no significant difference in the cell infiltration layer of both 0wt% and 7.5wt% groups after 6 weeks implantation, indicating that the degradation rates of both groups were similar and the degradation was dictated by the hydrolysis of ester bond between PEG and glutaric acid. Additionally, although cells could infiltrate into the pocket structure after the degradation of gelatin microgel, cell infiltration was still prevented by PEG adhesive. The results revealed that gelatin microgel containing PEG adhesive had the potential to promote cell infiltration if we could build a pathway with gelatin microgel for cells to go through the PEG adhesive.



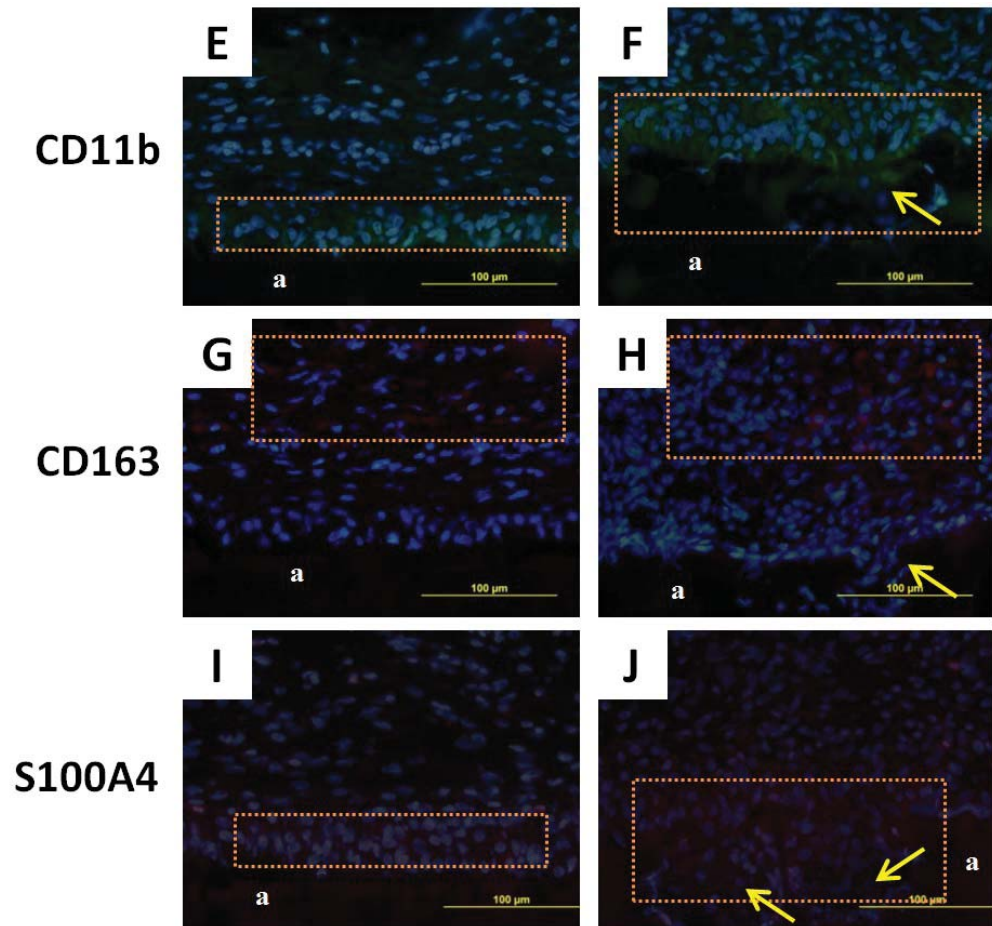
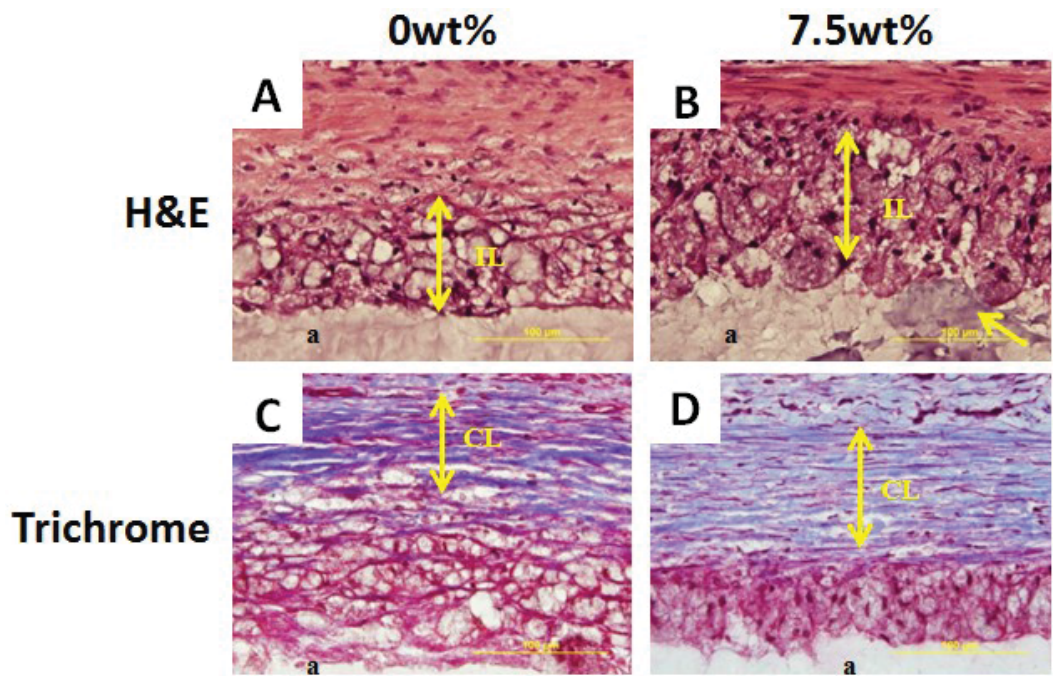


Figure 3-11. Hematoxylin and eosin stain (H&E stain) (A and B), Masson's Trichrome stain (C and D) and immunofluorescent stain (E-J) of 0wt% and 7.5wt% adhesive and surrounding tissue after 2 weeks subcutaneous implantation. a: adhesive; Orange box: cell distribution area. Single headed arrow: cell infiltrating into the pocket formed via gelatin microgel degradation. Blue (DAPI): cell nuclei; Green (CD11b): M1 macrophage; Red (CD163 and S100A4): M2 macrophage and fibroblast, respectively.





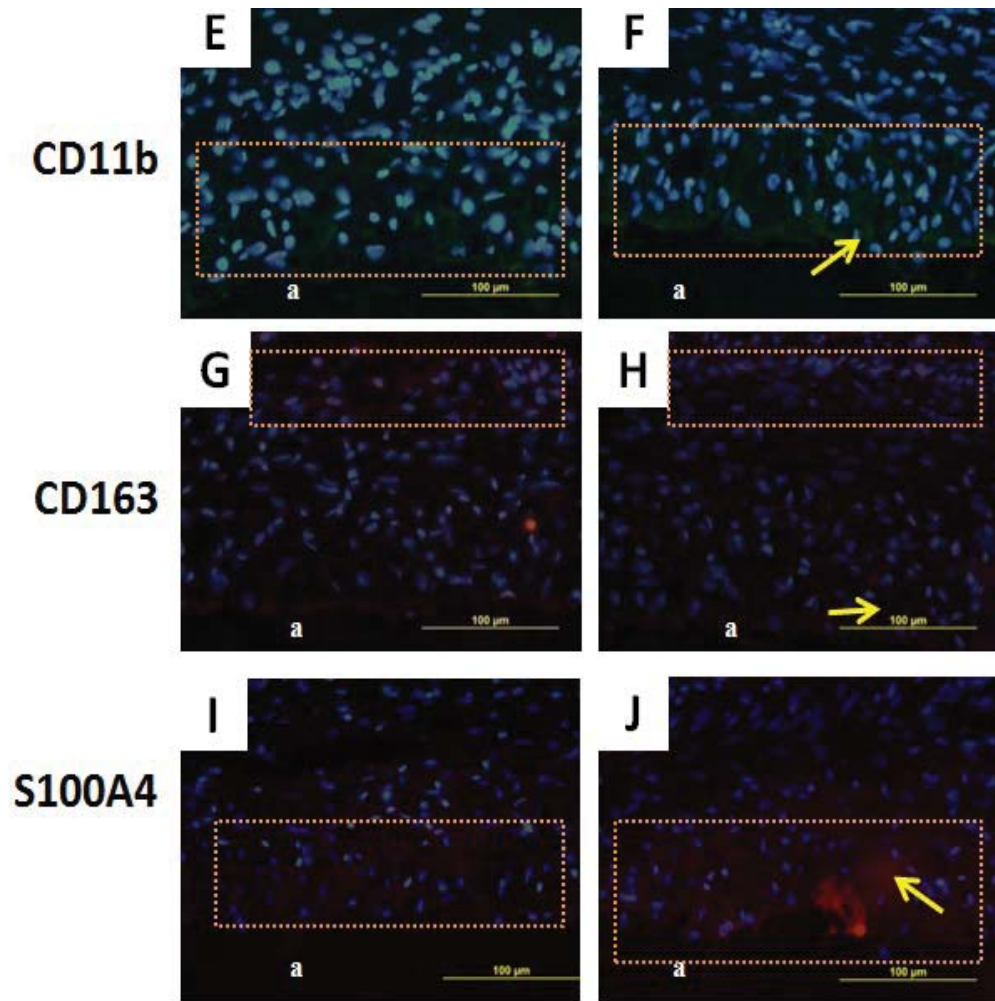


Figure 3-12. Hematoxylin and eosin stain (H&E stain) (A and B), Masson's Trichrome stain (C and D) and immunofluorescent stain (E-H) of 0wt% and 7.5wt% adhesive and surrounding tissue after 6 weeks subcutaneous implantation. a: adhesive; Orange box: cell distribution area. Single headed arrow: cell infiltrating into the pocket formed via gelatin microgel degradation. Double headed arrow : cell infiltration layer (IL in A and B) and collagen layer (CL in C and D), respectively. Blue (DAPI): cell nuclei; Green (CD11b): M1 macrophage; Red (CD163 and S100A4): M2 macrophage and fibroblast, respectively.

Table 3-2. Cell density, cell infiltration layer and collagen layer thickness of 2 weeks and 6 weeks subcutaneous implantation.

	2 weeks		6 weeks	
	0wt%	7.5wt%	0wt%	7.5wt%
Cell density in tissue-adhesive interface ( $\times 10^3$ cells/mm <sup>2</sup> )	5.3 $\pm$ 0.8	7.7 $\pm$ 0.9*	2.02 $\pm$ 0.66	3.4 $\pm$ 0.64*
Cell infiltration layer ( $\mu$ m)	-	-	95.79 $\pm$ 14.37	97.15 $\pm$ 16.78
Collagen layer thickness ( $\mu$ m)	-	-	43.63 $\pm$ 14.47	74.31 $\pm$ 14.14*

\* p < 0.05 when compared to 0wt% adhesive.

## 4. Conclusion

This study has demonstrated that PEG-GM adhesive presented improved adhesive property and enhanced bioactivity. PEG is known for its biocompatibility but the bioinert property makes it lacking of interaction with surrounding cells to regulate the cell function and tissue development.<sup>[4]</sup> The incorporation of gelatin microgel provided the cell binding sites to promote the bioactivity. In addition, the gelatin microgel reacted with PEGDM to form both chemical and physical bond to increase the bulk property of material. The incorporation of chemically crosslinked gelatin microgel into PEGDM also enhanced the mechanical stability of gelatin. The increasing weight percentage of



gelatin microgel contributed to a faster gelation of adhesive and showed stronger adhesive property under wet environment. The *in vitro* degradation test showed no significant difference among the adhesives with or without gelatin microgels, indicating that the adhesives degraded through the hydrolysis of ester bond between PEG and glutaric acid. Cell culture tests showed the PEG-GM adhesive as biocompatible and the addition of gelatin microgel enhanced the cell attachment and spreading on the adhesive surface. *In vivo* subcutaneous implantation test revealed that PEG-GM adhesive as biocompatible and bioactive. The higher deposition of collagen molecule made the PEG-GM adhesive a promising material for the wound healing of connective tissue.

In conclusion, incorporating gelatin microgel into PEGDM adhesive is a simple method to achieve an adhesive presenting enhanced adhesive property and bioactivity.

## **5. Future work**

Although cell infiltration can be observed in the present study, it is limited by the absence of efficient pathway for cell going through. In the future work it is possible to build an efficient pathway to further promote the cell infiltration. It is known that the stiffness of cell adhesion substrate will influence the cell response on the morphology

and adhesion.<sup>[88, 89]</sup> By changing the concentration of EDC and NHS the crosslinking density of gelatin gel can be controlled.<sup>[62]</sup> It is possible to control the cell response better through controlling the stiffness of gelatin microgel. We can also entrap growth factor molecule within the gelatin microgel. With the degradation of gelatin microgel, growth factor can be released to control the formation of normal and functional tissue. It is also necessary to build a new animal model to study the material as an injectable bioadhesive on tissue regeneration and wound healing.

## 6. Reference

- [1]. Uranüs S, Mischinger H-J, Pfeifer J, et al. Hemostatic methods for the management of spleen and liver injuries. *World J Surg* 1996; **20**(8): 1107-12.
- [2]. Li Y, Meng H, Liu Y, Lee BP. Fibrin Gel as an Injectable Biodegradable Scaffold and Cell Carrier for Tissue Engineering. *The Scientific World Journal* 2015; **2015**.
- [3]. Reid B, Gibson M, Singh A, et al. PEG hydrogel degradation and the role of the surrounding tissue environment. *J Tissue Eng Regen M* 2013.
- [4]. Shin H, Ruhe PQ, Mikos AG, Jansen JA. In vivo bone and soft tissue response to injectable, biodegradable oligo (poly (ethylene glycol) fumarate) hydrogels. *Biomaterials* 2003; **24**(19): 3201-11.
- [5]. Chung I-M, Enemchukwu NO, Khaja SD, Murthy N, Mantalaris A, García AJ. Bioadhesive hydrogel microenvironments to modulate epithelial morphogenesis. *Biomaterials* 2008; **29**(17): 2637-45.
- [6]. Shin H, Jo S, Mikos AG. Modulation of marrow stromal osteoblast adhesion on biomimetic oligo [poly (ethylene glycol) fumarate] hydrogels modified with Arg - Gly - Asp peptides and a poly (ethylene glycol) spacer. *Journal of biomedical materials research* 2002; **61**(2): 169-79.
- [7]. Hubbell JA, Massia SP, Desai NP, Drumheller PD. Endothelial cell-selective materials for tissue engineering in the vascular graft via a new receptor. *Nature Biotechnology* 1991; **9**(6): 568-72.
- [8]. Tabata Y, Ikada Y. Protein release from gelatin matrices. *Advanced drug delivery reviews* 1998; **31**(3): 287-301.
- [9]. Heris HK, Rahmat M, Mongeau L. Characterization of a hierarchical network of hyaluronic acid/gelatin composite for use as a smart injectable biomaterial. *Macromolecular bioscience* 2012; **12**(2): 202-10.
- [10]. Wu S-C, Chang W-H, Dong G-C, Chen K-Y, Chen Y-S, Yao C-H. Cell adhesion and proliferation enhancement by gelatin nanofiber scaffolds. *Journal of Bioactive and Compatible Polymers* 2011: 0883911511423563.
- [11]. Rosellini E, Cristallini C, Barbani N, Vozi G, Giusti P. Preparation and characterization of alginate/gelatin blend films for cardiac tissue engineering. *Journal of Biomedical Materials Research Part A* 2009; **91**(2): 447-53.
- [12]. Sung HW, Huang DM, Chang WH, Huang RN, Hsu JC. Evaluation of gelatin hydrogel crosslinked with various crosslinking agents as bioadhesives: in vitro study. *Journal of biomedical materials research* 1999; (46): 520-30.
- [13]. Bigi A, Cojazzi G, Panzavolta S, Rubini K, Roveri N. Mechanical and thermal properties of gelatin films at different degrees of glutaraldehyde crosslinking. *Biomaterials* 2001; **22**(8): 763-8.
- [14]. Vandelli M, Rivasi F, Guerra P, Forni F, Arletti R. Gelatin microspheres crosslinked with D, L-glyceraldehyde as a potential drug delivery system: preparation, characterisation, in vitro and in vivo studies. *International journal of pharmaceutics* 2001; **215**(1): 175-84.
- [15]. Kawai K, Suzuki S, Tabata Y, Ikada Y, Nishimura Y. Accelerated tissue regeneration through incorporation of basic fibroblast growth factor-impregnated gelatin microspheres into artificial dermis.

*Biomaterials* 2000; **21**(5): 489-99.

- [16]. Lee BP, Dalsin JL, Messersmith PB. Biomimetic adhesive polymers based on mussel adhesive proteins. *Biological Adhesives*: Springer; 2006: 257-78.
- [17]. Ehrbar M, Metters A, Zammaretti P, Hubbell JA, Zisch AH. Endothelial cell proliferation and progenitor maturation by fibrin-bound VEGF variants with differential susceptibilities to local cellular activity. *J Control Release* 2005; **101**(1): 93-109.
- [18]. Fortelny RH, Petter-Puchner AH, Glaser KS, Redl H. Use of fibrin sealant (Tisseel/Tissucol) in hernia repair: a systematic review. *Surgical endoscopy* 2012; **26**(7): 1803-12.
- [19]. Sanjay P, Watt DG, Wigmore SJ. Systematic review and meta-analysis of haemostatic and biliostatic efficacy of fibrin sealants in elective liver surgery. *J Gastrointest Surg* 2013; **17**(4): 829-36.
- [20]. Thumwanit V, Kedjarune U. Cytotoxicity of polymerized commercial cyanoacrylate adhesive on cultured human oral fibroblasts. *Australian dental journal* 1999; **44**(4): 248-52.
- [21]. Lumsden AB, Heyman ER, Group CMSSS. Prospective randomized study evaluating an absorbable cyanoacrylate for use in vascular reconstructions. *J Vasc Surg* 2006; **44**(5): 1002-9. e1.
- [22]. Maldonado T, Rosen R, Rockman C, et al. Initial successful management of type I endoleak after endovascular aortic aneurysm repair with n-butyl cyanoacrylate adhesive. *J Vasc Surg* 2003; **38**(4): 664-70.
- [23]. Losanoff JE, Richman BW, Jones JW. Cyanoacrylate adhesive in management of severe presacral bleeding. *Dis Colon Rectum* 2002; **45**(8): 1118-9.
- [24]. Shalaby SW. Polyester/cyanoacrylate tissue adhesive formulations. Google Patents; 2001.
- [25]. McCuen BW, Hida T, Sheta SM. Transvitreal cyanoacrylate retinopexy in the management of complicated retinal detachment. *Am J Ophthalmol* 1987; **104**(2): 127-32.
- [26]. Ferlise V, Ankem M, Barone J. Use of cyanoacrylate tissue adhesive under a diaper. *Bju Int* 2001; **87**(7): 672-3.
- [27]. Mattamal GJ. US FDA perspective on the regulations of medical-grade polymers: cyanoacrylate polymer medical device tissue adhesives. 2008.
- [28]. Zhu J. Bioactive modification of poly (ethylene glycol) hydrogels for tissue engineering. *Biomaterials* 2010; **31**(17): 4639-56.
- [29]. Jeon O, Samorezov JE, Alsberg E. Single and dual crosslinked oxidized methacrylated alginate/PEG hydrogels for bioadhesive applications. *Acta Biomater* 2014; **10**(1): 47-55.
- [30]. Burke SA, Ritter-Jones M, Lee BP, Messersmith PB. Thermal gelation and tissue adhesion of biomimetic hydrogels. *Biomedical materials* 2007; **2**(4): 203.
- [31]. Brubaker CE, Kissler H, Wang L-J, Kaufman DB, Messersmith PB. Biological performance of mussel-inspired adhesive in extrahepatic islet transplantation. *Biomaterials* 2010; **31**(3): 420-7.
- [32]. Lee BP, Messersmith PB, Israelachvili JN, Waite JH. Mussel-inspired adhesives and coatings. *Annual review of materials research* 2011; **41**: 99.
- [33]. Taylor SW, Chase DB, Emptage MH, Nelson MJ, Waite JH. Ferric ion complexes of a DOPA-containing adhesive protein from *Mytilus edulis*. *Inorganic Chemistry* 1996; **35**(26): 7572-7.
- [34]. Soriaga MP, Hubbard AT. Determination of the orientation of aromatic molecules adsorbed on

- platinum electrodes. The effect of solute concentration. *Journal of the American Chemical Society* 1982; **104**(14): 3937-45.
- [35]. Waite JH. Nature's underwater adhesive specialist. *International Journal of Adhesion and Adhesives* 1987; **7**(1): 9-14.
- [36]. Lee H, Scherer NF, Messersmith PB. Single-molecule mechanics of mussel adhesion. *Proceedings of the National Academy of Sciences* 2006; **103**(35): 12999-3003.
- [37]. Sugumaran M, Dali H, Semensi V. Chemical - and cuticular phenoloxidase - mediated synthesis of cysteinyl - catechol adducts. *Archives of Insect Biochemistry and Physiology* 1989; **11**(2): 127-37.
- [38]. Mizrahi B, Khoo X, Chiang HH, et al. Long-lasting antifouling coating from multi-armed polymer. *Langmuir : the ACS journal of surfaces and colloids* 2013; **29**(32): 10087-94.
- [39]. Zhu L-P, Yu J-Z, Xu Y-Y, Xi Z-Y, Zhu B-K. Surface modification of PVDF porous membranes via poly (DOPA) coating and heparin immobilization. *Colloids and Surfaces B: Biointerfaces* 2009; **69**(1): 152-5.
- [40]. Dalsin JL, Lin L, Tosatti S, Vörös J, Textor M, Messersmith PB. Protein resistance of titanium oxide surfaces modified by biologically inspired mPEG-DOPA. *Langmuir : the ACS journal of surfaces and colloids* 2005; **21**(2): 640-6.
- [41]. Moulay S. Dopa/Catechol-tethered polymers: Bioadhesives and biomimetic adhesive materials. *Polymer Reviews* 2014; **54**(3): 436-513.
- [42]. Laulicht B, Mancini A, Geman N, et al. Bioinspired Bioadhesive Polymers: Dopa - Modified Poly (acrylic acid) Derivatives. *Macromolecular bioscience* 2012; **12**(11): 1555-65.
- [43]. Choi YC, Choi JS, Jung YJ, Cho YW. Human gelatin tissue-adhesive hydrogels prepared by enzyme-mediated biosynthesis of DOPA and Fe<sup>3+</sup> ion crosslinking. *Journal of Materials Chemistry B* 2014; **2**(2): 201-9.
- [44]. Park K, Mrsny RJ. Controlled drug delivery: designing technologies for the future: ACS Books; 2000.
- [45]. Andrade J, Hlady V, Jeon S-I. Polyethylene oxide and protein resistance: principles, problems, and possibilities. *Polymeric Materials: Science and Engineering* 1993: 60-1.
- [46]. Nagaoka S, Nakao A. Clinical application of antithrombogenic hydrogel with long poly (ethylene oxide) chains. *Biomaterials* 1990; **11**(2): 119-21.
- [47]. Alcantar NA, Aydil ES, Israelachvili JN. Polyethylene glycol-coated biocompatible surfaces. *Journal of biomedical materials research* 2000; **51**(3): 343-51.
- [48]. Graham NB. Poly (ethylene oxide) and Related Hydrogels. *Hydrogels in medicine and pharmacy* 1987; **2**: 95-113.
- [49]. Peppas NA, Keys KB, Torres-Lugo M, Lowman AM. Poly (ethylene glycol)-containing hydrogels in drug delivery. *J Control Release* 1999; **62**(1): 81-7.
- [50]. Chang C-W, van Spreeuwel A, Zhang C, Varghese S. PEG/clay nanocomposite hydrogel: a mechanically robust tissue engineering scaffold. *Soft Matter* 2010; **6**(20): 5157-64.
- [51]. Hersel U, Dahmen C, Kessler H. RGD modified polymers: biomaterials for stimulated cell adhesion and beyond. *Biomaterials* 2003; **24**(24): 4385-415.
- [52]. Guarnieri D, De Capua A, Ventre M, et al. Covalently immobilized RGD gradient on PEG hydrogel scaffold influences cell migration parameters. *Acta Biomater* 2010; **6**(7): 2532-9.

- [53]. Burdick JA, Anseth KS. Photoencapsulation of osteoblasts in injectable RGD-modified PEG hydrogels for bone tissue engineering. *Biomaterials* 2002; **23**(22): 4315-23.
- [54]. te Nijenhuis K. Gelatin: Springer; 1997.
- [55]. Tomihata K, Burczak K, Shiraki K, Ikada Y. Cross-linking and biodegradation of native and denatured collagen. *Polymers of biological and biomedical significance* 1994; **540**: 275-86.
- [56]. Chvapil M. Collagen sponge: theory and practice of medical applications. *Journal of biomedical materials research* 1977; **11**(5): 721-41.
- [57]. Sela M, Arnon R. Studies on the chemical basis of the antigenicity of proteins. 1. Antigenicity of polypeptidyl gelatins. *Biochemical Journal* 1960; **75**(1): 91.
- [58]. Huang Y, Onyeri S, Siewe M, Moshfeghian A, Madihally SV. In vitro characterization of chitosan–gelatin scaffolds for tissue engineering. *Biomaterials* 2005; **26**(36): 7616-27.
- [59]. Ward AG, Courts A. Science and technology of gelatin: Academic Press; 1977.
- [60]. Djabourov M, Papon P. Influence of thermal treatments on the structure and stability of gelatin gels. *Polymer* 1983; **24**(5): 537-42.
- [61]. de Carvalho W, Djabourov M. Physical gelation under shear for gelatin gels. *Rheologica Acta* 1997; **36**(6): 591-609.
- [62]. Kuijpers A, Engbers G, Feijen J, et al. Characterization of the network structure of carbodiimide cross-linked gelatin gels. *Macromolecules* 1999; **32**(10): 3325-33.
- [63]. Kuijpers A, Van Wachem P, Van Luyn M, et al. In vivo compatibility and degradation of crosslinked gelatin gels incorporated in knitted Dacron. *Journal of biomedical materials research* 2000; **51**(1): 136-45.
- [64]. Nakayama Y, Matsuda T. Photocurable surgical tissue adhesive glues composed of photoreactive gelatin and poly (ethylene glycol) diacrylate. *Journal of biomedical materials research* 1999; **48**(4): 511-21.
- [65]. Balakrishnan B, Joshi N, Jayakrishnan A, Banerjee R. Self-crosslinked oxidized alginate/gelatin hydrogel as injectable, adhesive biomimetic scaffolds for cartilage regeneration. *Acta Biomater* 2014; **10**(8): 3650-63.
- [66]. Wu H, Zhang Z, Wu D, Zhao H, Yu K, Hou Z. Preparation and drug release characteristics of pingyangmycin - loaded dextran cross - linked gelatin microspheres for embolization therapy. *Journal of Biomedical Materials Research Part B: Applied Biomaterials* 2006; **78**(1): 56-62.
- [67]. Martin P. Wound healing--aiming for perfect skin regeneration. *Science* 1997; **276**(5309): 75-81.
- [68]. Velnar T, Bailey T, Smrkolj V. The wound healing process: an overview of the cellular and molecular mechanisms. *J Int Med Res* 2009; **37**(5): 1528-42.
- [69]. Gabbiani G. The myofibroblast in wound healing and fibrocontractive diseases. *The Journal of pathology* 2003; **200**(4): 500-3.
- [70]. Montesano R, Orci L. Transforming growth factor beta stimulates collagen-matrix contraction by fibroblasts: implications for wound healing. *Proceedings of the National Academy of Sciences* 1988; **85**(13): 4894-7.
- [71]. Tomasek JJ, Gabbiani G, Hinz B, Chaponnier C, Brown RA. Myofibroblasts and mechano-regulation of connective tissue remodelling. *Nature Reviews Molecular Cell Biology* 2002; **3**(5): 349-63.

- [72]. Meng H, Li Y, Faust M, Konst S, Lee BP. Hydrogen peroxide generation and biocompatibility of hydrogel-bound mussel adhesive moiety. *Acta Biomater* 2015; **17**: 160-9.
- [73]. Lee BP, Dalsin JL, Messersmith PB. Synthesis and gelation of DOPA-modified poly (ethylene glycol) hydrogels. *Biomacromolecules* 2002; **3**(5): 1038-47.
- [74]. Liu Y, Zhan H, Skelton S, Lee BP. Marine Adhesive Containing Nanocomposite Hydrogel with Enhanced Materials and Bioadhesive Properties. *MRS Proceedings*; 2013: Cambridge Univ Press; 2013. p. mrss13-1569-II05-09.
- [75]. Liu Y, Meng H, Konst S, Sarmiento R, Rajachar R, Lee BP. Injectable Dopamine-Modified Poly (ethylene glycol) Nanocomposite Hydrogel with Enhanced Adhesive Property and Bioactivity. *ACS applied materials & interfaces* 2014; **6**(19): 16982-92.
- [76]. Yun EJ, Yon B, Joo MK, Jeong B. Cell therapy for skin wound using fibroblast encapsulated poly (ethylene glycol)-poly (l-alanine) thermogel. *Biomacromolecules* 2012; **13**(4): 1106-11.
- [77]. Brown BN, Valentin JE, Stewart-Akers AM, McCabe GP, Badylak SF. Macrophage phenotype and remodeling outcomes in response to biologic scaffolds with and without a cellular component. *Biomaterials* 2009; **30**(8): 1482-91.
- [78]. Mehdizadeh M, Weng H, Gyawali D, Tang L, Yang J. Injectable citrate-based mussel-inspired tissue bioadhesives with high wet strength for sutureless wound closure. *Biomaterials* 2012; **33**(32): 7972-83.
- [79]. Cencer M, Liu Y, Winter A, Murley M, Meng H, Lee BP. Effect of pH on the Rate of Curing and Bioadhesive Properties of Dopamine Functionalized Poly (ethylene glycol) Hydrogels. *Biomacromolecules* 2014; **15**(8): 2861-9.
- [80]. Anseth KS, Bowman CN, Brannon-Peppas L. Mechanical properties of hydrogels and their experimental determination. *Biomaterials* 1996; **17**(17): 1647-57.
- [81]. Ding X, Vegesna GK, Meng H, Winter A, Lee BP. Nitro - Group Functionalization of Dopamine and its Contribution to the Viscoelastic Properties of Catechol - Containing Nanocomposite Hydrogels. *Macromolecular Chemistry and Physics* 2015; **216**(10): 1109-19.
- [82]. Ding X, Vegesna GK, Meng H, Winter A, Lee BP. Nitro - Group Functionalization of Dopamine and its Contribution to the Viscoelastic Properties of Catechol - Containing Nanocomposite Hydrogels. *Macromolecular Chemistry and Physics* 2015.
- [83]. Skelton S, Bostwick M, O'Connor K, Konst S, Casey S, Lee BP. Biomimetic adhesive containing nanocomposite hydrogel with enhanced materials properties. *Soft Matter* 2013; **9**(14): 3825-33.
- [84]. Brubaker CE, Messersmith PB. Enzymatically degradable mussel-inspired adhesive hydrogel. *Biomacromolecules* 2011; **12**(12): 4326-34.
- [85]. Schmedlen RH, Masters KS, West JL. Photocrosslinkable polyvinyl alcohol hydrogels that can be modified with cell adhesion peptides for use in tissue engineering. *Biomaterials* 2002; **23**(22): 4325-32.
- [86]. Giancotti FG. Complexity and specificity of integrin signalling. *Nature Cell Biology* 2000; **2**(1): E13-E4.
- [87]. Chen CS, Mrksich M, Huang S, Whitesides GM, Ingber DE. Geometric control of cell life and death. *Science* 1997; **276**(5317): 1425-8.
- [88]. Discher DE, Janmey P, Wang Y-I. Tissue cells feel and respond to the stiffness of their substrate.

*Science* 2005; **310**(5751): 1139-43.

[89]. Yeung T, Georges PC, Flanagan LA, et al. Effects of substrate stiffness on cell morphology, cytoskeletal structure, and adhesion. *Cell motility and the cytoskeleton* 2005; **60**(1): 24-34.

[90]. Marchant R, Hiltner A, Hamlin C, Rabinovitch A, Slobodkin R, Anderson JM. In vivo biocompatibility studies. I. The cage implant system and a biodegradable hydrogel. *Journal of biomedical materials research* 1983; **17**(2): 301-25.

[91]. Anderson JM, Miller KM. Biomaterial biocompatibility and the macrophage. *Biomaterials* 1984; **5**(1): 5-10.

[92]. Tabata Y, Ikada Y. Macrophage activation through phagocytosis of muramyl dipeptide encapsulated in gelatin microspheres. *Journal of pharmacy and pharmacology* 1987; **39**(9): 698-704.

[93]. Diegelmann RF, Evans MC. Wound healing: an overview of acute, fibrotic and delayed healing. *Front Biosci* 2004; **9**(1): 283-9.

[94]. Badylak SF, Valentin JE, Ravindra AK, McCabe GP, Stewart-Akers AM. Macrophage phenotype as a determinant of biologic scaffold remodeling. *Tissue Engineering Part A* 2008; **14**(11): 1835-42.

[95]. Guo S, DiPietro LA. Factors affecting wound healing. *Journal of dental research* 2010; **89**(3): 219-29.

[96]. Gosain A, DiPietro LA. Aging and wound healing. *World J Surg* 2004; **28**(3): 321-6.

[97]. Anderson JM, Rodriguez A, Chang DT. Foreign body reaction to biomaterials. *Seminars in immunology*; 2008: Elsevier; 2008. p. 86-100.

[98]. Anderson JM, Shive MS. Biodegradation and biocompatibility of PLA and PLGA microspheres. *Advanced drug delivery reviews* 2012; **64**: 72-82.



# Appendix

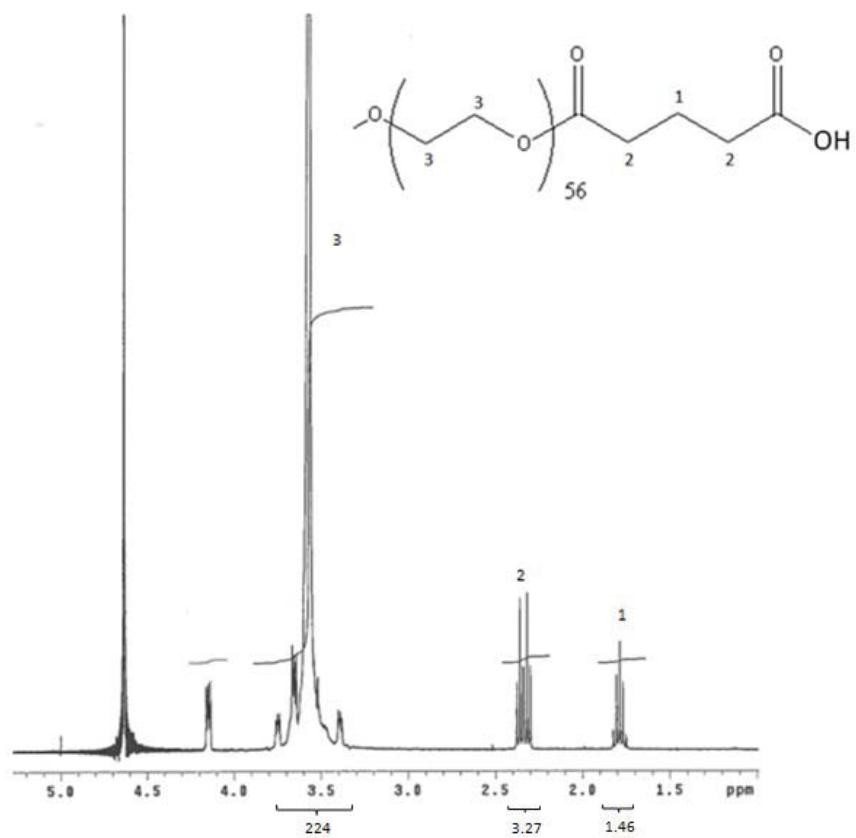


Figure A1. NMR spectrum of PEGGlu.

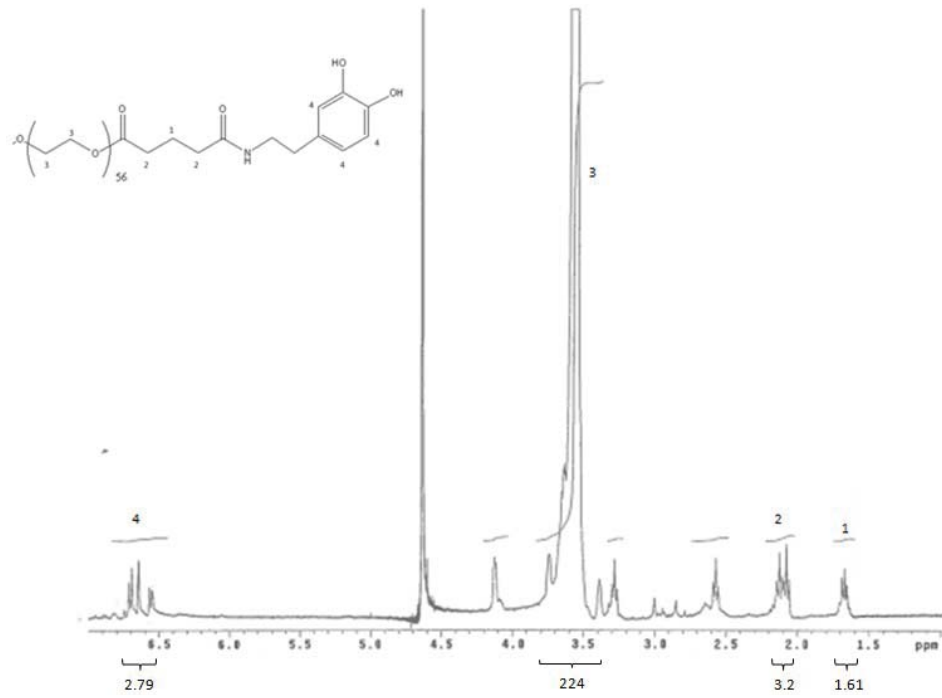


Figure A2. NMR spectrum of PEGDM.

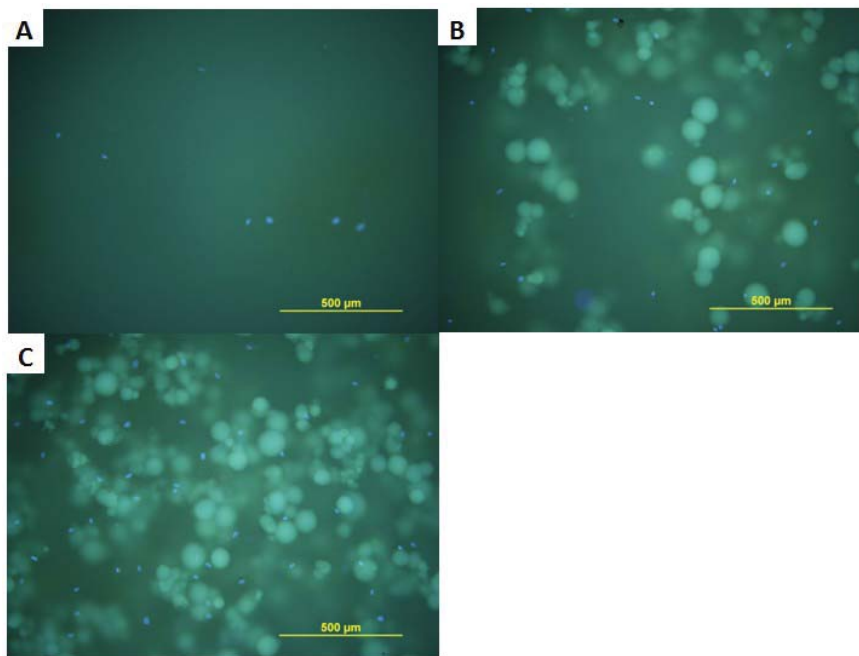


Figure A3. DAPI staining of rat dermal fibroblasts for cell attachment test. A) 0wt% adhesive; B) 3.75wt% adhesive; 7.5wt% adhesive. Small blue dots: cell nuclei; Large cyan dots: gelatin microgels.

Table A1. Compression test results of crosslinked bulk gelatin gel.

Failure stress kPa	Failure strain	Elastic modulus kPa	Toughness kJ/m <sup>3</sup>
563±51.5	0.53±0.03	128±9.8	218±6.3

## Copyright permission for Figure 1-3



RightsLink®

Home

Create Account

Help



**Title:** Mussel-Inspired Adhesives and Coatings  
**Author:** Bruce P. Lee, P.B. Messersmith, J.N. Israelachvili, et al  
**Publication:** Annual Review of Materials Research  
**Publisher:** Annual Reviews  
**Date:** Aug 4, 2011  
Copyright © 2011, Annual Reviews

LOGIN

If you're a [copyright.com](#) user, you can login to RightsLink using your [copyright.com](#) credentials. Already a [RightsLink](#) user or want to [learn more?](#)

### Permission Not Required

Material may be republished in a thesis / dissertation without obtaining additional permission from Annual Reviews, providing that the author and the original source of publication are fully acknowledged.

BACK

CLOSE WINDOW

Copyright © 2015 [Copyright Clearance Center, Inc.](#) All Rights Reserved. [Privacy statement](#). [Terms and Conditions](#).

Comments? We would like to hear from you. E-mail us at [customercare@copyright.com](mailto:customercare@copyright.com)

## Copyright permission for Figure 1-6

15-7-28

RightsLink® by Copyright Clearance Center



# RightsLink®

Home

Create Account

Help



ACS Publications  
Most Trusted. Most Cited. Most Read.

**Title:** Characterization of the Network Structure of Carbodiimide Cross-Linked Gelatin Gels  
**Author:** A. J. Kuijpers, G. H. M. Engbers, J. Feijen, et al  
**Publication:** Macromolecules  
**Publisher:** American Chemical Society  
**Date:** May 1, 1999  
Copyright © 1999, American Chemical Society

LOGIN

If you're a [copyright.com](#) user, you can login to RightsLink using your [copyright.com](#) credentials. Already a [RightsLink](#) user or want to [learn more?](#)

### PERMISSION/LICENSE IS GRANTED FOR YOUR ORDER AT NO CHARGE

This type of permission/license, instead of the standard Terms & Conditions, is sent to you because no fee is being charged for your order. Please note the following:

- Permission is granted for your request in both print and electronic formats, and translations.
- If figures and/or tables were requested, they may be adapted or used in part.
- Please print this page for your records and send a copy of it to your publisher/graduate school.
- Appropriate credit for the requested material should be given as follows: "Reprinted (adapted) with permission from (COMPLETE REFERENCE CITATION). Copyright (YEAR) American Chemical Society." Insert appropriate information in place of the capitalized words.
- One-time permission is granted only for the use specified in your request. No additional uses are granted (such as derivative works or other editions). For any other uses, please submit a new request.

If credit is given to another source for the material you requested, permission must be obtained from that source.

BACK

CLOSE WINDOW

Copyright © 2015 [Copyright Clearance Center, Inc.](#) All Rights Reserved. [Privacy statement.](#) [Terms and Conditions.](#)

Comments? We would like to hear from you. E-mail us at [customer@copyright.com](mailto:customer@copyright.com)